CHEMBIOCHEM

Supporting Information

Modulating Protein–Protein Interactions with Visible-Light-Responsive Peptide Backbone Photoswitches

Lea Albert,[a] Alberto Peñalver,[a] Nemanja Djokovic,[b] Laura Werel,[a] Malte Hoffarth,[a] Dusan Ruzic,[b] Jing Xu,[c] Lars-Oliver Essen,[a] Katarina Nikolic,[b] Yali Dou,[c] and Olalla Vázquez*[a]

cbic_201800737_sm_miscellaneous_information.pdf

Table of Contents

Abbreviations

ε	extinction coefficient
λ	wavelength
v	frequency
A	anisotropy
a.u.	aberration units
Ahx	aminohexanoic acid
Alloc	alkyloxycarbonyl
Azo	azobenzene
Boc	*tert*-butylcarbonyl
c	concentration
cAzo	cyclic azobenzene
calcd.	calculated
conc.	concentration
CuCN	copper (I) cyanide
DBU	1,8-diazabicyclo[5,4,0]undeca-7-ene
DIC	*N, N'*-diisopropylcarbodiimide
DIPEA	*N, N'*-diisopropylethylamine
DMF	*N, N'*-dimethylformamide
DMSO	dimethyl sulfoxide
DTT	dithiotheitrol
E. coli	*Escherichia coli*
EtOAc	ethyl acetate
EDTA	ethylenediaminetetraacetic acid
ESI	electrospray ionization
eq.	equivalents

oF_4Azo	tetra-*ortho*-fluorazobenzene
FAM	fluorescein
Fmoc	fluorenylmethyloxycarbonyl chloride
FP	fluorescence polarization
GSH	glutathione
HFIP	hexafluoroisopropanol
HMT	histone methyltransferase
HPLC	high-performance liquid chromatography
HRMS	high resolution mass spectrometry
IC_{50}	half inhibitory concentration
IPTG	isopropyl β-D-1-thiogalactopyranoside
irr.	irradiation
K_d	dissociation constant
K_i	inhibition constant
M	molar
mAU	milli absorbance units
MD	Molecular Dynamics
MLL1	mixed lineage leukaemia 1
mP	milli polarization value
MPD	2-methyl-2,4-pentanediol
Mtt	4-methyltrityl
NMP	*N*-methyl-2-pyrrolidon
NMR	nuclear magnetic resonance
Ni-NTA	nickel nitrilotriacetic acid
PMSF	phenylmethylsulfonyl fluoride
PSS	photostationary state

PyBop	benzotriazol-1-yl-oxytripyrrolidinophosphonium hexafluorophosphate
R_f	retention factor
RbBP5	retinoblasma-bindin-protein 5
RP	reversed phase
rpm	revolutions per minute
r.t.	room temperature
SAM	S-adenosylmethionine
sec.	seconds
SPPS	solid phase peptide synthesis
t_0	time zero
t_R	retention time
TFA	trifluoroacetic acid
THF	tetrahydrofuran
TLC	thin layer chromatography
TIS	triisopropyl silane
Tris	tris(hydroxymethyl)aminomethane
Trt	trityl
UV	ultraviolet
vis	visible
WDR5	WD-repeat protein-5

Experimental Procedures

Materials

All commercially reagents were purchased from the following companies and used without further purification: DMSO biograde, NaCl biograde, Tris, 2-mercaptoethanol, Fmoc-Cl, $FeSO_4$ × 7 H_2O and DIPEA from Carl Roth (Germany); 6-aminohexanoic acid and $KMnO_4$ from Alfa Aesar (Germany); OxymaPure from Luxembourg Bio Technologies (Israel); DIC, ammonium persulfate and glycerol from Acros (USA); Sieber amide resin, Mtt-Cl, 4-bromo-2,6-difluoraniline and MBHA resin from Fluorochem (UK); glucose monohydrate from Applichem (Germany); CuCN and HCl from TCI (Japan); PyBop from Novabiochem (Germany); KCl biograde, Triton, 2-Cl-Trt resin, $NaNO_3$, NaOH, KOH, 4,4'-ethylenedianiline, IPTG, ampicillin and dithiothreitol from Goldbio (USA); LB-broth, LB-agar, bromphenolblue and Tween-20 from Thermo Fisher (USA); $ZnSO_4$ from Fluka (USA); acrylamide from National diagnostics (USA); glutathione-sepharose beads from GE-Healthcare (USA); protease inhibitor from Roche diagnostics (Germany), S-adenosylmethionine from Biolabs (USA); *tert*-butyl-2-bromoacetate, ethylenediamine, PMSF, kanamycin, NP-40 and $MgSO_4$, from Sigma Aldrich/ Merck (Germany); Fmoc-protected amino acids, DMF peptide grade, HATU and TentaGel S RAM resin from Iris Biotech (Germany); MeCN HPLC grade, pyridine, H_2SO_4 and triethylamine from VWR (France). The $H3_{1-21}$ peptide and dimethylated $H3_{1-21}$ peptide were purchased from Anaspec (USA, ref. codes: AS-61702; AS-64356); The protein marker (ref. nr.: 1610373) and BSA stocks (ref. nr.: 500-0207) from Bio-Rad (USA). The plasmid preparation kit was purchased from Quiagen (ref. code: 27106, USA) and the corresponding mini-prep column from Denville Scientific (ref. nr.: CM-400-250, USA). Beads and buffers used for AlphaLISA Assay were purchased from Perkin Elmer (USA): 5 × buffer: AlphaLISA 5 × epigenetics buffer 1 (AL008F1); 30 × buffer: AlphaLISA 30 × epigenetics buffer supplement (AL008L2); acceptor bead: AlphaLISA anti-H3K4me1-2 acceptor beads (AL116M); donor beads: AlphaScreen streptavidin donor beads (6760002). Water was purified with a Milli-Q Ultra Pure Water Purification System (TKA, Germany).

Nuclear Magnetic Resonance Spectroscopy (NMR)

NMR spectra were recorded at 300 K either on a Bruker AV III HD 300 MHz at a frequency of 300 MHz (^{1}H), 75 MHz (^{13}C, ^{13}C-APT) or on a Bruker AV III HD 500 MHz at a frequency of 500 MHz (^{1}H), 125 MHz (^{13}C) or on a Bruker AV III HD 600 MHz at a frequency of 600 MHz (^{1}H). The ^{1}H, ^{13}C and ^{13}C-APT NMR spectra were referenced to solvent residue peaks. As internal standards, deuterated chloroform ($CDCl_3$), deuterated dimethyl sulfoxide ([D_6]DMSO) with TMS or deuterated water (D_2O) were used. Solvent shifts (ppm): ($CDCl_3$, δ) = 7.26 ppm (^{1}H) and 77.16 ppm (^{13}C), ([D_6]DMSO, δ) = 2.50 ppm (^{1}H) and 39.52 (^{13}C), D_2O = 4.79 ppm (^{1}H).

Mass Spectrometry

High resolution electrospray ionization (ESI) mass spectra were acquired with a LTQ-FT Ultra mass spectrometer (Thermo Fischer Scientific). The resolution was set to 100,000. Field desorption (FD) time-of-Flight (FD-TOF/MS) mass spectra were acquired with an AccuTOF GCv 4G (JEOL) Time of Flight (TOF) mass spectrometer. FD-emitters were purchased from Linden ChroMasSpec GmbH (Bremen, Germany).

High Performance Liquid Chromatography (HPLC)

For preparative purposes, a PLC 2020 Personal Purification System (Gilson) with a preparative Nucleodur C18 HTec-column (5 µm, 250 x 16 mm; Macherey & Nagel) with a flow rate of 10 mL/min or a semipreparative C18 3001 coulumn (Phenomenex) with a flow rate of 8 mL/min using an isocratic regime during the first five minutes, for column equilibration, followed by the respectively stated linear gradient in 30 min at 25°C. The detection was carried out by measuring the absorption at wavelengths: 220 nm and 260 nm. Milli-Q water (A) and MeCN (B) were employed as eluents with an addition of 0.1% of TFA in both solvents.

Analytical HPLC-MS were recorded on an Agilent 1200 Series HPLC-system (Agilent Technologies), with a column oven set to 55 °C. Detection was monitored at 220 nm. Milli-Q water (A) and MeCN (B) were employed as eluents with an addition of 0.05% and 0.03% of TFA. Different analytical columns and methods were used:

- column 1: EC 125/2 Nucleodur 100-C18 ec column (Macherey & Nagel) using the stated linear gradient in 30 min with a flow rate of 0.20 mL/min
- column 2: Eclipse XBD-C18 column (Agilent Technologies) using the stated linear gradient in 30 min with a flow rate of 1.00 mL/min
- column 3: Kinetex 5µm XB-C18 100Å LC column 150 × 4.6 mm (Phenomenex) using the stated linear gradient in 30 min with a flow rate of 1.00 mL/min

UV-Vis Spectroscopy

Concentration determinations and UV-vis measurements were performed on a Tecan (Switzerland) Spark 20M multimode microplate reader at r.t. All measurements were performed in a 1400 µL quartz cuvette (Hellma Analytics (104F-QS) with a pathlength of 1 cm. The, to be measured, compound was added to 700 uL of the respective blank measurement in the cuvette and absorbance spectra were recorded. To determine the concentration of the peptides the following extinction coefficients were used: *o*F_4Azo-containing peptides (for *trans* isomer) ε_{319} = 25000 L mol^{-1} cm^{-1} in MeCN,[1] cAzo-containing peptides (for *cis* isomer) ε_{238} = 25990 L mol^{-1} cm^{-1} in MilliQ water, fluorescently tagged peptides ε_{494} = 76900 L mol^{-1} cm^{-1} in 0.1 M phosphate buffer, pH = 9[2]).

Photoisomerization of *o*F_4Azo and cAzo Peptides

For isomerization an UV-Emitter 405 nm SMD Roschwege Star-UV405-03-00-00, 3 W (to reach the *trans* photostationary state) and a HighPower-LED Green 87 lm 130° 3.8 V, 1000 mA Roschwege (to reach the *cis* photostationary state) were used for irradiation at 405 and 525 nm, respectively. For the irradiation at 525 nm an additional cut-on filter (OG515 coloured glass filter, 515 nm longpass, Thorlabs) was applied. Experiments were performed at r.t.

Fluoresence Polarization-based Assay

All FP-based assays were performed at r.t. in black 96-well microtiter plates (Greiner) and the FP was measured as milipolarization (mP) units on a Tecan (Switzerland) Spark 20M multimode microplate reader; settings: used filters, excitation: 485 nm; emission: 530 nm; gain: optimal; Z-position: calculated from control well (0% inhibition: tracer and protein in assay

buffer); number of flashes: 30; G-factor: 1.067. The data evaluation was done, using GraphPad Prism 6 software.

Competitive Fluorescence Polarization-based Binding Assay

The binding affinities of both isomers of each peptide were measured separately as reported by us previously.[3] The isomerization, however, was done differently as detailed above. The peptides were dissolved in DMSO biograde. In order to calculate the binding affinity of the *trans* isomers, the peptide solutions were irradiated at 405 nm for 10 sec. To determine the binding affinity of the *cis* isomers, the peptide solutions were irradiated at 525 nm for 2 min in a transparent glass vial, previously to the assay. Afterwards, the whole assay had to be done in darkness to prevent *cis* → *trans* and *trans* → *cis* relaxation. 120 µL of a preincubated complex solution of WDR5Δ23 and the tracer peptide in assay buffer (0.1 M phosphate buffer pH = 6.5, 25 mM KCl, 0.01% Triton) were added to 5 µL of dilutions of the respective peptide in DMSO in triplicate, reaching the final concentrations of 72 nM for WDR5Δ23 and 20 nM for the tracer peptide. Three control wells in triplicate were included in each plate: blank (without tracer and protein), 100% inhibition (tracer only) and 0% inhibition (protein and tracer). The plates were incubated on a shaker (Edmund Bühler TiMix Control TH15) at r.t. for 5 h and the mP values were recorded. GraphPad Prism 6 software was used for data evaluation. K_i values were calculated using the following equation described previously by Wang et al. and the corresponding webpage provided by them:[4]

$$K_i = \frac{[I]_{50}}{\frac{[L]_{50}}{K_d} + \frac{[P]_0}{K_d} + 1}$$

where $[I]_{50}$ denotes the concentration of the free inhibitor at 50 % inhibition, $[L]_{50}$ is the concentration of free labelled ligand at 50 % inhibition, $[P]_0$ is the concentration of the free protein at 0 % inhibition, and K_d is the dissociation constant of the protein-ligand complex.

Transformation, Expression and Purification of Proteins

Cultivation of Pre-cultures

Pre-cultures of the pET28 plasmids of WDR5Δ23, MLL1(3762-end), Ash2L (1-534), RbBP5 (1-538) and the pGEX plasmid of GST-MLL1, used for inoculation of heterologous expression and starting material for plasmid preparation were prepared in test tubes with 5.00 mL LB medium with kanamycin for the pETH28 plasmids and with ampicillin for the pGEX plasmid. Then, either a colony from a plate or some cell material from a glycerol stock was scratched off with a toothpick and added to the test tube. The culture was incubated on a shaker at 37 °C with 200 rpm for 16 h. For better oxygen transfer, test tubes were attached in an inclined way. Glycerol stocks were prepared by mixing 700 µL preculture with 300 µL 80% glycerol. They were flash frozen in liquid nitrogen and stored at -80 °C.

Transformation

Transformation was performed thawing aliquots of competent *E. coli* BL21 codon + cells on ice. To 25 µL of these cells, 1 µL of the respective plasmids were added. The mixture was incubated for 30 min on ice, followed by a heat shock in a 42 °C water bath for 45 sec. After

2 min incubation on ice, 250 µL of LB medium was added and the suspension was shaken at 37 °C, 200 rpm for 1 h. Then, 50 µL were plated on LB-agar-kanamycin/ampicillin plates and incubated for 16 h at 37 °C.

Plasmid Preparation

The plasmid preparation was performed by the use of the Quiagen kit (see Materials section). Therefore, a 5.00 mL culture is prepared with the particular plasmid containing cells and incubated at 37 °C for 16 h. After harvesting the cells, the pellet is lysed with 250 µL resuspension buffer P1, which consists of RNAse that cleaves RNA and EDTA, which complexes the cations that normally stabilize the cell membrane. By adding 250 µL lysis buffer P2, which contains SDS and NaOH to disrupt the cell membrane and denatures dsDNA. Due to their *supercoil* structure, plasmids are, in contrast to genomic DNA, able to recover the denaturation. After mixing and incubation for 5 min, 350 µL neutralization buffer N3 was added. Such buffer containing KOAc, neutralizes the pH and leads to precipitation of chromosomal DNA and proteins. The precipitant is pelleted during a 10 min centrifugation (13000 rpm) step. The supernatant is then transferred onto a small column, washed once with 500 µL PB buffer, once with 750 µL PE buffer and finally eluted with 30 µL EB buffer or MilliQ water. Concentrations were measured photometric at 260 nm, which is the absorption maxima of nucleic acids.

Expression and Purification of His-SUMO tagged Proteins

The pET28a-based His-Sumo-Proteins (WDR5Δ23, MLL1 (3762-end), Ash2L (1-534), RbBP5 (1-538)) were expressed from the pET28-MHL vector in *E. coli* BL21 codon+ cells. Expression was performed by inoculation of 800 mL LB medium into 2 L baffled flasks with 50 µg/mL kanamycin and 50 mL of pre-culture. For the expression of MLL1 and Ash2L, $ZnSO_4$ in MilliQ water to a final concentration of 10 µM was added to ensure proper folding of the enzyme. The culture was incubated on a shaker (Multitron from Infors HT) at 37 °C and 200 rpm until an OD_{600} of 0.5-0.6 was reached. The temperature was then reduced to 20 °C and the expression was induced by adding IPTG up to a final concentration of 0.3 mM. The cells were grown for 16 h and harvested through centrifugation (5000 rpm, 15 min, 4 °C, Sorvall RC6 Plus from Thermo Scientific). The cell pellet from the 800 mL expression culture was resuspended in 40 mL lysis buffer (400 µL PMSF (stock: 100 mM), 400 µL 10% NP-40, 4 µL 2-mercaptoethanole and one tablet of protease inhibitor (Roche diagnostics) cocktail in 40 mL BC500). Lysis of the cells was carried out using a sonicator Sonoplus HD 220 from Bandelin (3 x 40%, output: 4, with 2 min pulses and 3 min rest). After sonification, the suspension was pelleted by centrifugation (12000 rpm, 20 min, 4 °C). The lysate was added to Ni-NTA agarose (Quiagen, Germany) and incubated for 1 h at 4 °C. Cleavage of the His_6-tag was achieved by incubation of the resin with 3.0 mL BC500 + 18.1 µL ULP-His_6. Proteins used for the HMT-Assay were used without further purification.

WDR5Δ23 used for the FP-binding assays and for crystallization was further purified by loading onto a Mono S 5/50 GL column (GE Healthcare) using an ÄKTA purification system (GE Healthcare). The flow rate was 1 mL/min with the Mono S buffers A (25 mM Tris, pH = 8.0, 20% glycerol) and B (25 mM Tris, pH = 8.0, 1 M NaCl, 20% glycerol) with first an isocratic flow of 100% A for 10 min followed by a linear gradient of 0-100% B in 20 min. WDR5Δ23 eluted between 35-40% of buffer B. The fractions were checked via SDS-PAGE and pooled. The

buffer was changed to the dialysis buffer (25 mM Tris, pH = 8.0, 150 mM NaCl) and the protein was concentrated to 200 µM. The concentrated protein was aliquoted, flash frozen in liquid nitrogen and stored at -80 °C.

Expression and Purification of GST tagged Proteins

The pGEX-based GST-proteins were expressed in *E. coli* BL21 codon+ cells. Expression was performed by inoculation of 800 mL LB medium into 2 L baffled flasks with 50 µg/mL ampicillin and 50 mL of pre-culture. For the expression of GST-MLL1, 10 µM $ZnSO_4$ was added to ensure proper folding of the enzyme. The culture was incubated on a shaker (Multitron from Infors HT) at 37 °C and 200 rpm until an OD_{600} of 0.5-0.6 was reached. The temperature was then reduced to 20 °C and the expression was induced by adding IPTG up to a final concentration of 0.2 mM. The cells were grown for 16 h and harvested through centrifugation (5000 rpm, 15 min, 4 °C, Sorvall RC6 Plus from Thermo Scientific). The cell pellet from the 800 mL expression culture was resuspended in 40 mL lysis buffer (400 µL PMSF (stock: 100 mM), 400 µL 10% NP-40, 4 µL 2-mercaptoethanole and one tablet of protease inhibitor cocktail in 40 mL BC350 (25 mM Tris, pH = 8.0, 350 mM NaCl, 20% glycerol)). Lysis of the cells was carried out using a sonicator Sonoplus HD 220 from Bandelin (3 x 40%, output: 4, with 2 min pulses and 3 min rest). After sonification, the suspension was pelleted by centrifugation (12000 rpm, 20 min, 4 °C). The lysate was added to glutathione-sepharose beads (GE Healthcare, USA) and incubated for 1 h at 4 °C. Cleavage of the GST-tag was achieved by incubation of the resin with 1.0 mL BC350 + 10 µM reduced glutathione for 1 h at 4°C. This step was repeated twice. Finally, the protein was dialysed with BC-350 without glycerol to wash out remaining glutathione.

Synthesis

The names of the chemical compounds were generated with ChemDraw Professional (2017, Perkin Elmer). The commercial compounds do not have numbers, only the synthesized ones.

Synthesis of Fmoc-protected cyclic azobenzene amino acid (Fmoc-cAzoAA, 1)

The retrosynthesis route of the **Fmoc-cAzoAA 1** is illustrated in Scheme S1. In the Supporting Information only the procedures for the literature reported compounds are shown. The procedures for the novel compounds are detailed in the Manuscript, and the NMR spectra are shown here in the Supporting Information.

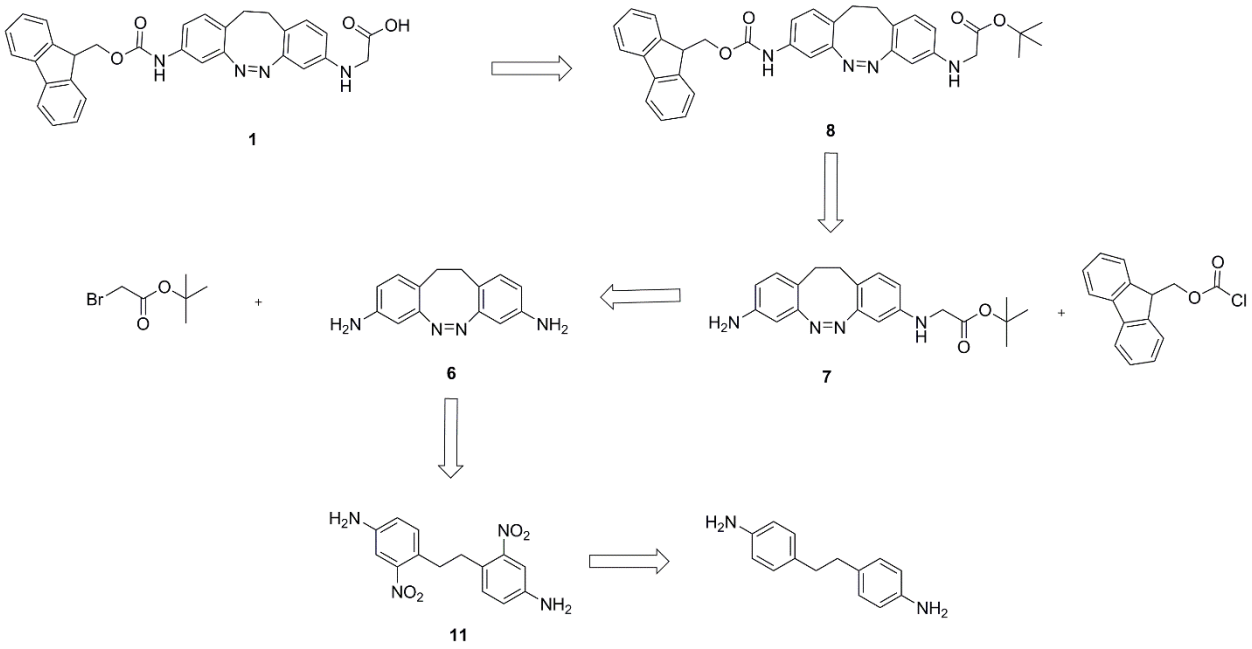

Scheme S1. Retrosynthesis route of the Fmoc-protected cyclic azobenzene amino acid **1** (**Fmoc-cAzoAA**).

4,4'-(ethane-1,2-diyl)bis(3-nitroaniline) (**11**)

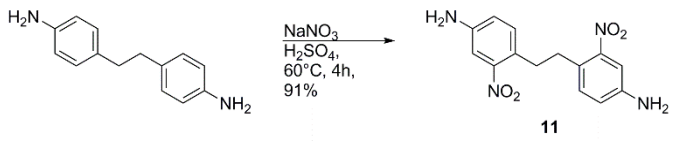

Scheme S2. Nitration of 1,2-bis(4-aminophenyl)ethane to the compound **11**.

Following the procedure of Sell at al.[5], the 1,2-bis(4-aminophenyl)ethane (1.00 g, 4.71 mmol, 1.00 eq.) was dissolved in 8.50 mL H_2SO_4 (conc.) and was heated to 60 °C. A solution of $NaNO_3$ (881 mg, 10.4 mmol, 2.20 eq.) in 9.10 mL of H_2SO_4 (conc.) was added. After stirring at

60 °C for 4 h the solution was poured into 100 mL of ice water. The resulting green suspension was neutralized by the addition of an aqueous ammonia solution (25%). The orange precipitate was filtered off, washed with distilled water and dried in vacuo. The product **11** was obtained as an orange solid (1.30 g, 4.30 mmol, 91%). The characterization is in agreement with the literature.[5] **TLC:** R_f = 0.05 (CH_2Cl_2/MeOH 1:1 + 1% NEt_3) **^{1}H NMR (300 MHz, DMSO, δ):** 7.06 (d, ^3J = 2.4 Hz, 2H, 2 × CH_{ar}), 6.99 (d, ^3J = 8.3 Hz, 2H, 2 × CH_{ar}), 6.80 (d, ^3J = 2.4 Hz, 1H, CH_{ar}), 6.77 (d, ^3J = 2.4 Hz, 1H, CH_{ar}), 5.58 (s, 4H, 2 × NH_2), 2.86 (s, 4H, 2 × CH_2). **^{13}C NMR (75 MHz, DMSO, δ):** 149.4 (2 × C_{ar}), 148.1 (2 × C_{ar}), 132.3 (2 × C_{ar}), 121.4 (2 × C_{ar}), 118.8 (2 × C_{ar}), 108.0 (2 × C_{ar}), 32.7 (2 × CH_2). **HRMS-ESI+ (m/z):** calcd. for $[M+Na]^+$ $C_{14}H_{14}N_4O_4Na$: 325.0907; found: 325.0901.

(*Z*)-11,12-dihydrodibenzo[c,g][1,2]diazocine-3,8-diamine (**6**)

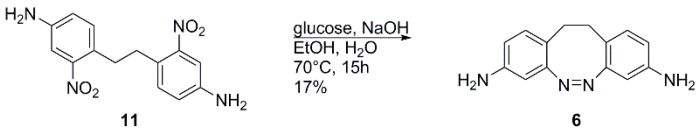

Scheme S3. Cyclization to form the cAzo derivative **6**.

Following the procedure of Sell at al.[5], compound **11** (800 mg, 2.65 mmol, 1.00 eq.) was dissolved in 106 mL EtOH. NaOH (6.65 g, 166 mmol, 62.8 eq.) in 26.5 mL distilled water was added and the mixture was warmed up to 70 °C. Then, glucose monohydrate (5.39 g, 27.2 mmol, 10.3 eq.) in 15 mL of distilled water was added. The solution was stirred at 70 °C for 15 h. The reaction was quenched by addition of 250 mL distilled water. The product was extracted with EtOAc (6 × 100 mL), washed with brine and dried over anhydrous $MgSO_4$. The crude was purified by flash column chromatography (pentane/EtOAc 1:1). The product **6** was obtained as a yellow solid (107.5 mg, 0.451 mmol, 17%). The characterization is in agreement with the literature.[5] **TLC:** R_f = 0.38 (pentane/EtOAc 1:1) **^{1}H NMR (300 MHz, $CDCl_3$, δ):** 6.73 (d, ^3J = 8.1 Hz, 2H, 2 × CH_{ar}), 6.35 (d, ^3J = 2.4 Hz, 1H, CH_{ar}), 6.32 (d, ^3J = 2.4 Hz, 1H, CH_{ar}), 6.14 (d, ^3J = 2.4 Hz, 2H, 2 × CH_{ar}), 3.55 (s, 4H, 2 × NH_2), 2.85.2.78 (m, 2H CH_2), 2.62-2.55 (m, 2H CH_2). **^{13}C NMR (75 MHz, $CDCl_3$, δ):** 156.4 (2 × C_{ar}), 144.9 (2 × C_{ar}), 130.6 (2 × CH_{ar}), 118.6 (2 × C_{ar}), 114.2 (2 × CH_{ar}), 105.3 (2 × CH_{ar}), 31.2 (2 × CH_2). **HRMS-ESI+ (m/z):** calcd. for $[M+H]^+$ $C_{14}H_{14}N_4H$: 239.1291; found: 239.1291.

NMRs of tert-butyl (Z)-(8-amino-11,12-dihydrodibenzo[c,g][1,2]diazocin-3-yl)glycinat (**7**)

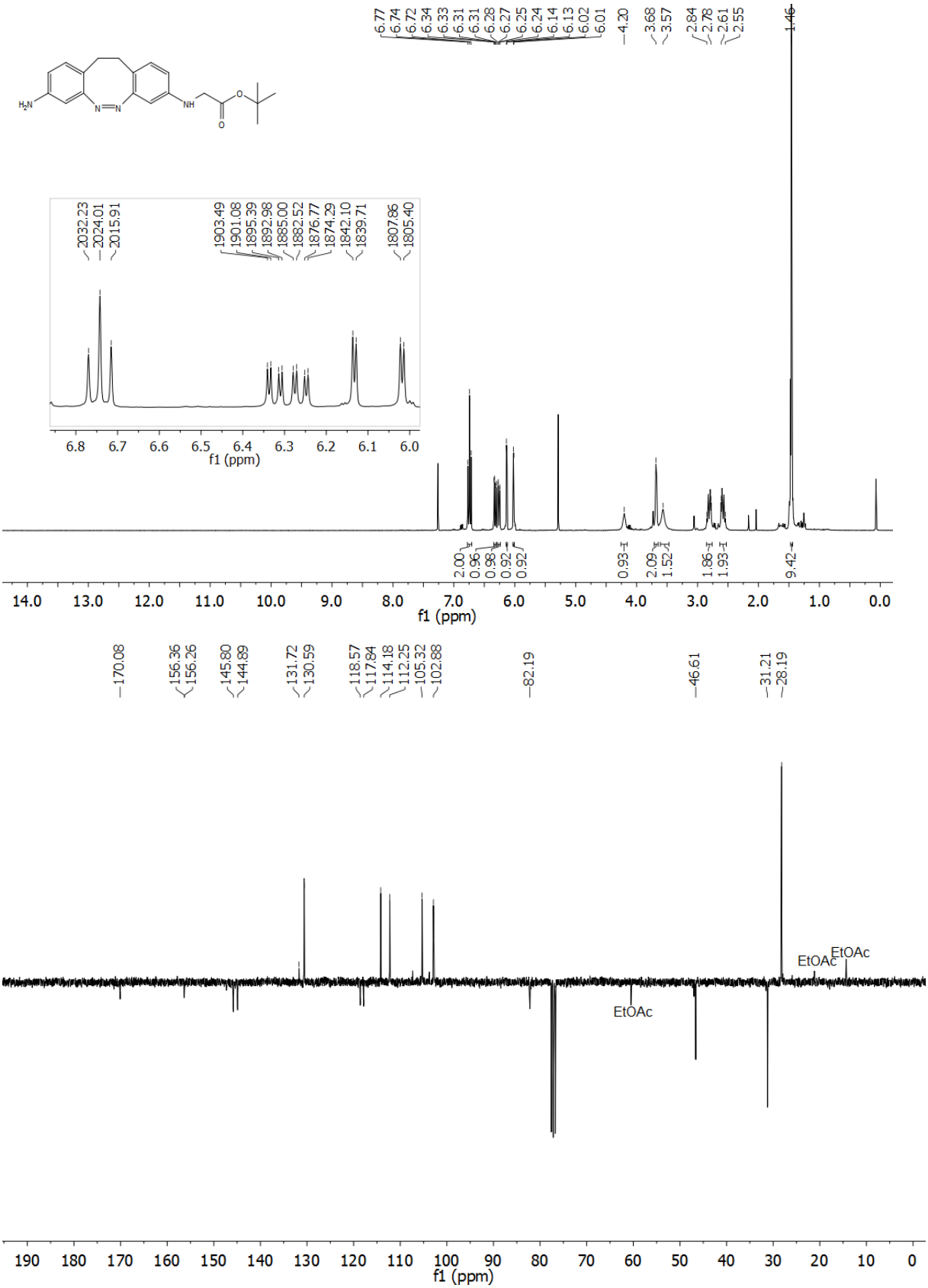

Figure S1. Top: ^{1}H-NMR spectrum of the compound **7**. Insert: zoom of signals in the aromatic region to highlight the shifts in Hz units for calculating *J*-constants. Bottom: ^{13}C-APT-NMR spectrum of compound **7**.

NMRs of tert-butyl (Z)-(8-Fmoc-11,12-dihydrodibenzo[c,g][1,2]diazocin-3-yl)glycinate (**8**)

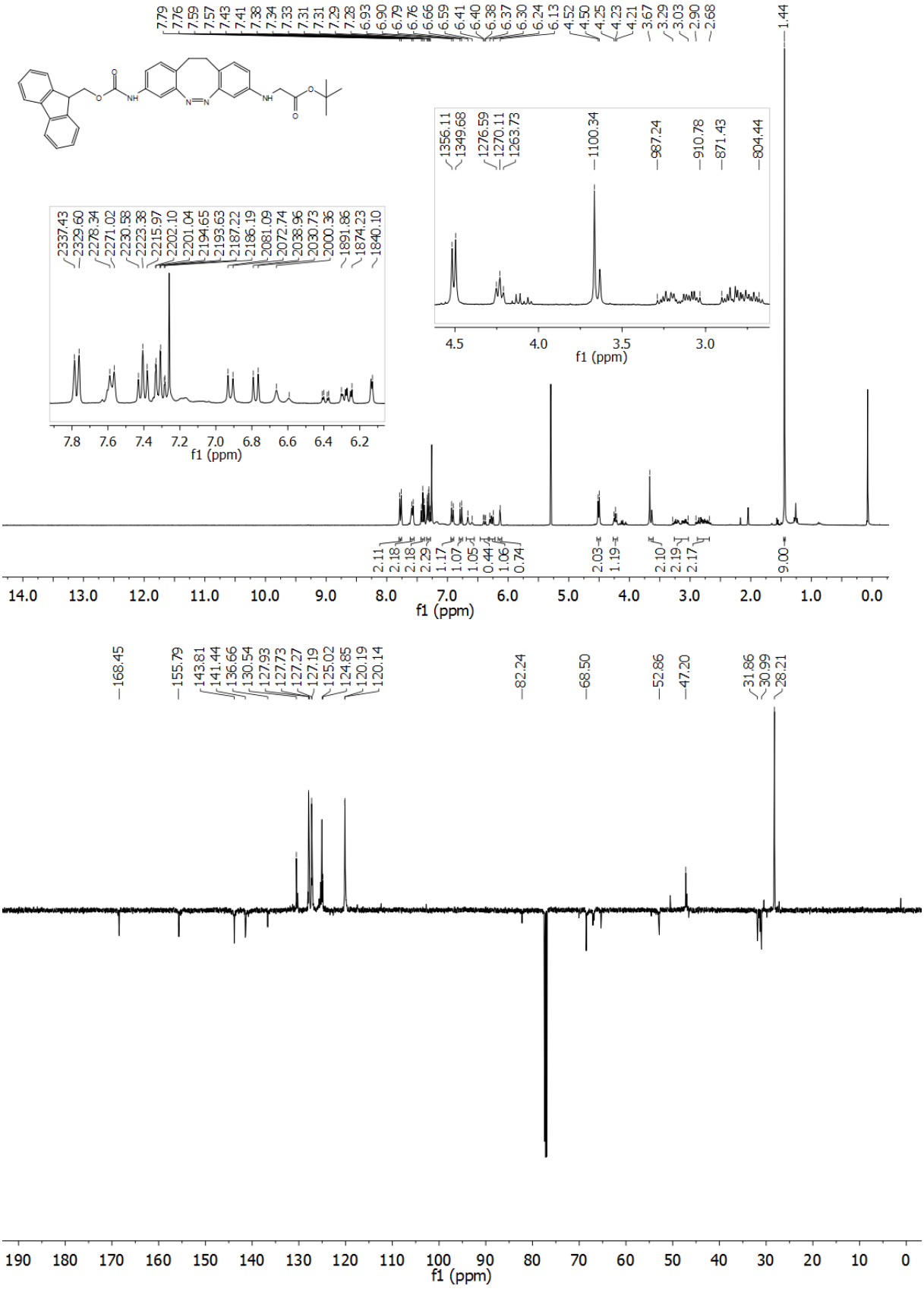

Figure S2. Top: ^{1}H-NMR spectrum of the compound **8**. Insert: zoom-in of signals in the aromatic and CH region to highlight the shifts in Hz units for calculating *J*-constants. Bottom: ^{13}C-APT-NMR spectrum of compound **8**.

NMRs of (*Z*)-(8-Fmoc-11,12-dihydrodibenzo-[c,g][1,2]diazocin-3-yl)glycinate (**1**)

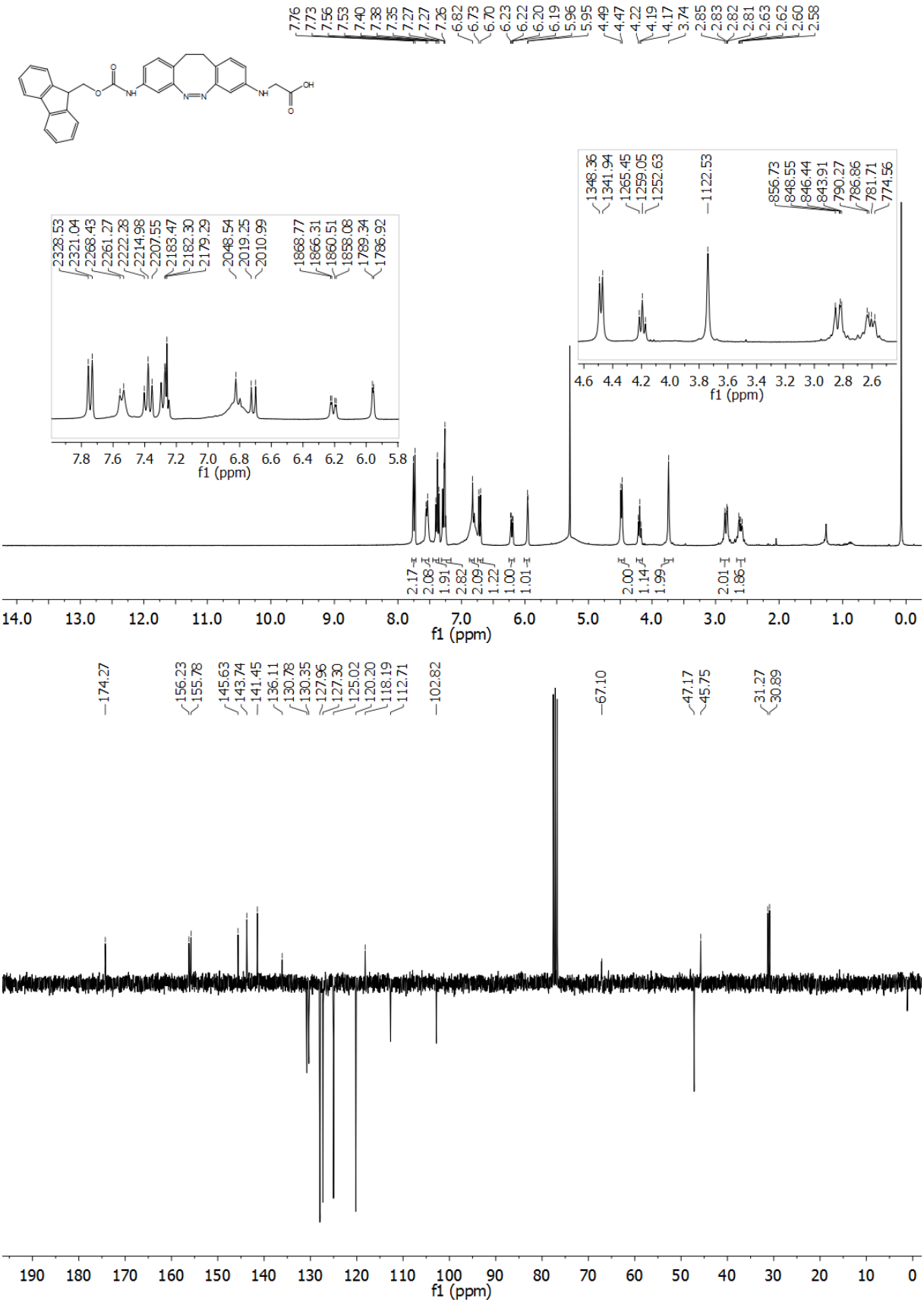

Figure S3. Top: ^{1}H-NMR spectrum of the compound **1**. Insert: zoom-in of signals in the aromatic and CH region to highlight the shifts in Hz units for calculating *J*-constants. Bottom: ^{13}C-APT-NMR spectrum of compound **1**.

Synthesis of Mtt-protected tetra-*ortho*-fluoroazobenze amino acid (Mtt-*o*F$_4$AzoAA, 2)

The retrosynthesis route of **Mtt-*o*F$_4$AzoAA** (**2**) is illustrated in Scheme S4. In the Supporting Information only the procedures for the literature reported compounds are shown. The procedures for the novel compounds are detailed in the Manuscript, and the NMR spectra are shown here in the Supporting Information.

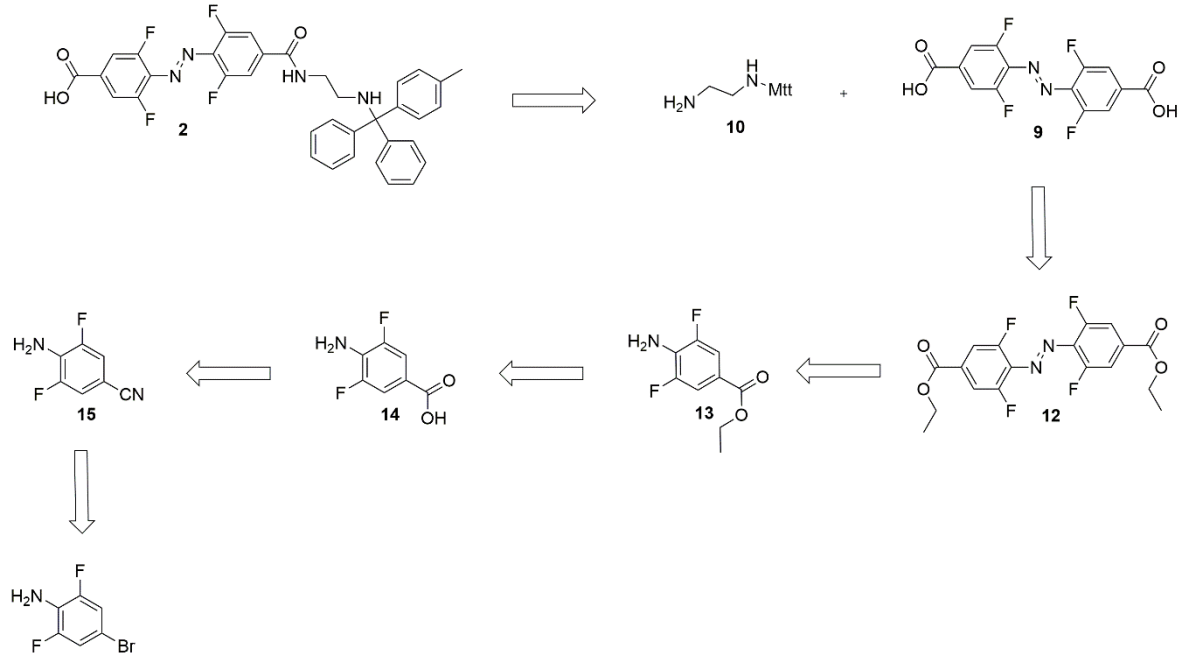

Scheme S4. Retrosynthesis route for the Mtt-protected tetra-*ortho*-fluoroazobenzene amino acid (**2**) (**Mtt-*o*F$_4$AzoAA**).

4-amino-3,5-difluorobenzonitrile (**15**)

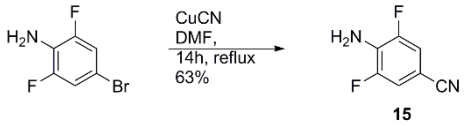

Scheme S5. Synthesis of *o*F$_2$Azo derivative **15**.

Following the procedure of Bléger et al.[6], the 4-bromo-2,6-difluoroaniline (5.00 g, 24.0 mmol, 1.00 eq.) and CuCN (6.45 g, 72.0 mmol, 3.00 eq.) were dissolved in 50.0 mL DMF and heated to 160 °C for 16 h. After cooling to r.t., the mixture was poured into a NH_3 aqueous solution (12 %, 250 mL), filtered and the precipitate was washed serveral times with EtOAc. The organic phases were washed with the same NH_3 solution, distilled water, brine and dried over anhydrous $MgSO_4$. The crude was purified by flash column chromatography (CH_2Cl_2/*n*-pentane 2:1) to yield the product **15** (2.33 g, 15.1 mmol, 63%) as a white solid. **TLC:** R_f = 0.39 (CH_2Cl_2/pentane 2:1). The characterization is in agreement with the literature.[6] **^{1}H NMR (300 MHz, $CDCl_3$, δ):** 7.13 (dd, ^3J = 6.0 Hz, ^4J = 2.2 Hz, 2H, 2 × CH_{ar}), 4.29 (s, 2H, NH_2). **^{13}C NMR (75 MHz, $CDCl_3$, δ):** 152.3 (FC_{ar}), 149.1 (FC_{ar}), 129.7(C_{ar}), 118.0 (*C*N), 115.7 (C_{ar}H), 115.4 (C_{ar}H); 98.4 (C_{ar}). **HRMS-EI+ (m/z):** calcd. for $[M+H]^+$ $C_7H_4F_2N_2$, 154.03425; found, 154.03252.

4-amino-3,5-difluorobenzoic acid (**14**)

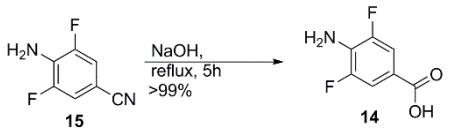

Scheme S6. Synthesis of *o*F_2Azo derivative **14**.

Following the procedure of Bléger et al.[6], the 4-amino-3,5-difluorobenzonitrile (**15**, 1.99 g, 12.9 mmol, 1.00 eq.) was suspended in 1 M NaOH (80.0 mL) and stirred at 110 °C for 4 h. The reaction mixture was cooled to r.t. and afterwards acidified with 1 M HCl (10.0 mL). The resulting precipitate was filtered, washed with distilled water and dried to yield the desired product **14** (2.23 g, 12.9 mmol, 99%) as a white solid. The characterization is in agreement with the literature.[6] **^{1}H NMR (300 MHz, DMSO-d$_6$, *δ*):** 12.68 (s, 1H, COOH), 7.40 (dd, $^3J_{HH}$ 7.2, $^4J_{HH}$ 2.5, 2H, 2 × CH_{ar}), 6.05 (s, 2H, NH_2). **^{13}C NMR (75 MHz, DMSO-d$_6$, *δ*):** 166.0 (*C*OOH), 151.3 (FC_{ar}), 148.2 (FC_{ar}), 130.6 (C_{ar}), 115.6 ($C_{ar.}$), 112.3 (C_{ar}H), 112.1 (C_{ar}H). **HRMS-ESI-(m/z):** calcd. for $[M-H]^-$ $C_7H_4F_2N_1O_2$, 172.0216; found, 172.0217.

ethyl 4-amino-3,5-difluorobenzoate (**13**)

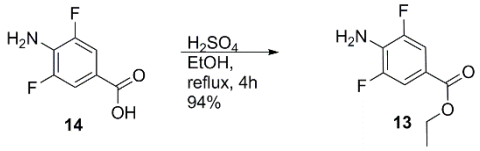

Scheme S7. Synthesis of *o*F_2Azo derivative **13**.

Following the procedure of Bléger et al.,[6] the 4-amino-3,5-difluorobenzoic acid (**14**, 1.90 g, 11.0 mmol, 1.00 eq.) was dissolved in EtOH (40.0 mL) and conc. H_2SO_4 (6.00 mL) and refluxed for 6 h. The solution was neutralized with saturated $NaHCO_3$, extracted with CH_2Cl_2, dried over anhydrous $MgSO_4$, filtered and the solvent was removed under reduced pressure to yield the desired product (**13**, 2.07 g, 10.3 mmol, 94%) as a pale brown solid. The characterization is in agreement with the literature.[6] **^{1}H NMR (300 MHz, CDCl$_3$, *δ*):** 7.53 (dd, ^3J = 7.2 Hz, ^4J = 2.1 Hz, 2H, 2 × CH_{ar}), 4.33 (q, ^3J = 7.1 Hz, 2H, OCH_2), 3.86 (s, 2 H, NH_2), 1.37 (t, ^3J = 7.1, 3H, CH_3). **^{13}C NMR (75 MHz, CDCl$_3$, *δ*):** 165.3 (*C*O), 152.4 (FC_{ar}), 149.3 (FC_{ar}), 128.9 ($C_{ar.}$), 118.8 ($C_{ar.}$), 112.8 (C_{ar}H), 112.6 (C_{ar}H), 61.2 (CH_2), 14.5 (CH_3). **HRMS-ESI+ (m/z):** calcd. for $[M+H]^+$ $C_9H_9F_2N_1O_2H$, 202.0674; found, 202.0675.

Diethyl 4,4'-(diazene-1,2-diyl)-bis(3,5-difluorobenzoate) (**12**)

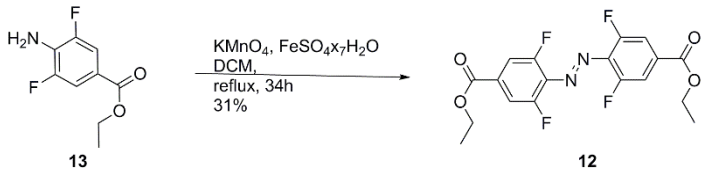

13 12

Scheme S8. Synthesis of the *o*F$_4$Azo derivative **12**.

Following the procedure of Bléger et al.[6], the ethyl-4-amino-3,5-difluorobenzoate (**13**, 2.43 g, 12.1 mmol, 1.00 eq.) was dissolved in CH_2Cl_2 (300 mL) and $KMnO_4$ (20.0 g, 127 mmol, 10.5 eq) and $FeSO_4$ x 7 H_2O (20.0 g, 71.9 mmol, 5.94 eq.) were added. The reaction mixture was refluxed for 28 h and filtered over celite. The solvent was removed under reduced pressure and the crude was purified by flash column chromatography (CH_2Cl_2/pentane 1:1) to yield the desired product **12** (748 mg, 1.88 mmol, 31%) as a red solid. The characterization is in agreement with the literature.[6] **TLC:** R_f = 0.75 (CH_2Cl_2); **^{1}H NMR (300 MHz, $CDCl_3$, δ):** 7.75 (d, ^3J = 8.9 Hz, 4H, 4 × CH_{ar}), 4.43 (q, ^3J = 7.1 Hz, 4H, 2 × CH_2), 1.43 (t, ^3J =7.1 Hz, 6H, 2 × CH_3).**^{13}C NMR (75 MHz, $CDCl_3$, δ):** 163.8 (2 × *C*O), 156.9 (2 × C_{ar}), 153.4 (2 × C_{ar}), 134.0 (2 × C_{ar}), 133.9 (2 × C_{ar}), 114.2 (2 × C_{ar}), 113.9 (2 × C_{ar}), 62.3 (2 × *C*H$_2$), 14.3 (2 × *C*H$_3$). **HRMS-ESI+ (m/z):** calcd. for $[M+H]^+$ $C_{18}H_{14}F_4N_2O_4H$, 399.0962; found: 399.0963.

Diethyl 4,4'-(diazene-1,2-diyl)-bis(3,5-difluorobenzoate) (**9**)

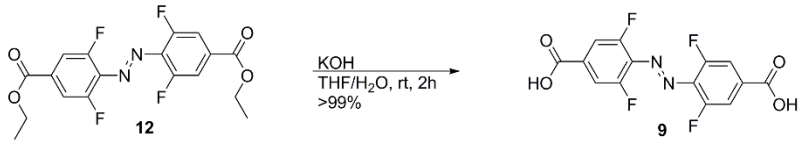

12 9

Scheme S9. Synthesis of *o*F$_4$Azo derivative **9**.

Following the procedure of Bléger et al.[7], the diethyl 4,4'-(diazene-1,2-diyl)-bis(3,5-difluorobenzoate) (**12**, 457 mg, 1.22 mmol, 1.00 eq.) was dissolved in THF (30.0 mL) and a solution of KOH (242 mg, 4.31 mmol, 3.53 eq.) in distilled water (15.0 mL) was added. The reaction mixture was stirred for 4 h, and then acidified with 1 M HCl (5.00 mL). The formed precipitate was filtered, washed with distilled water and dried on the freeze drier for 10 h to yield the desired product **9** (417 mg, 1.22 mmol, <99%) as a red solid. The characterization is in agreement with the literature.[7] **^{1}H NMR (300 MHz, DMSO-d$_6$, δ):** 13.91 (s, 2H, 2 × COO*H*), 7.82 (d, ^3J = 9.3 Hz, 4H, 4 × CH_{ar}). **^{13}C NMR (75 MHz, DMSO-d$_6$, δ):** 164.5 (2 × *C*O), 156.0 (2 × C_{ar}), 152.5 (2 × C_{ar}), 135.2 (2 × C_{ar}), 133.0 (2 × C_{ar}), 114.0 (2 × C_{ar}), 113.7 (2 × C_{ar}). **HRMS-ESI- (m/z):** calcd. for $[M-H]^-$ $C_{14}H_5F_4N_2O_4$, 341.0191; found, 341.0203.

NMR of 4-((4-((2-((diphenyl(p-tolyl)methyl)amino)ethyl)carbamoyl)-2,6-difluorophenyl) diazenyl) -3,5-difluorobenzoic acid (**2**)

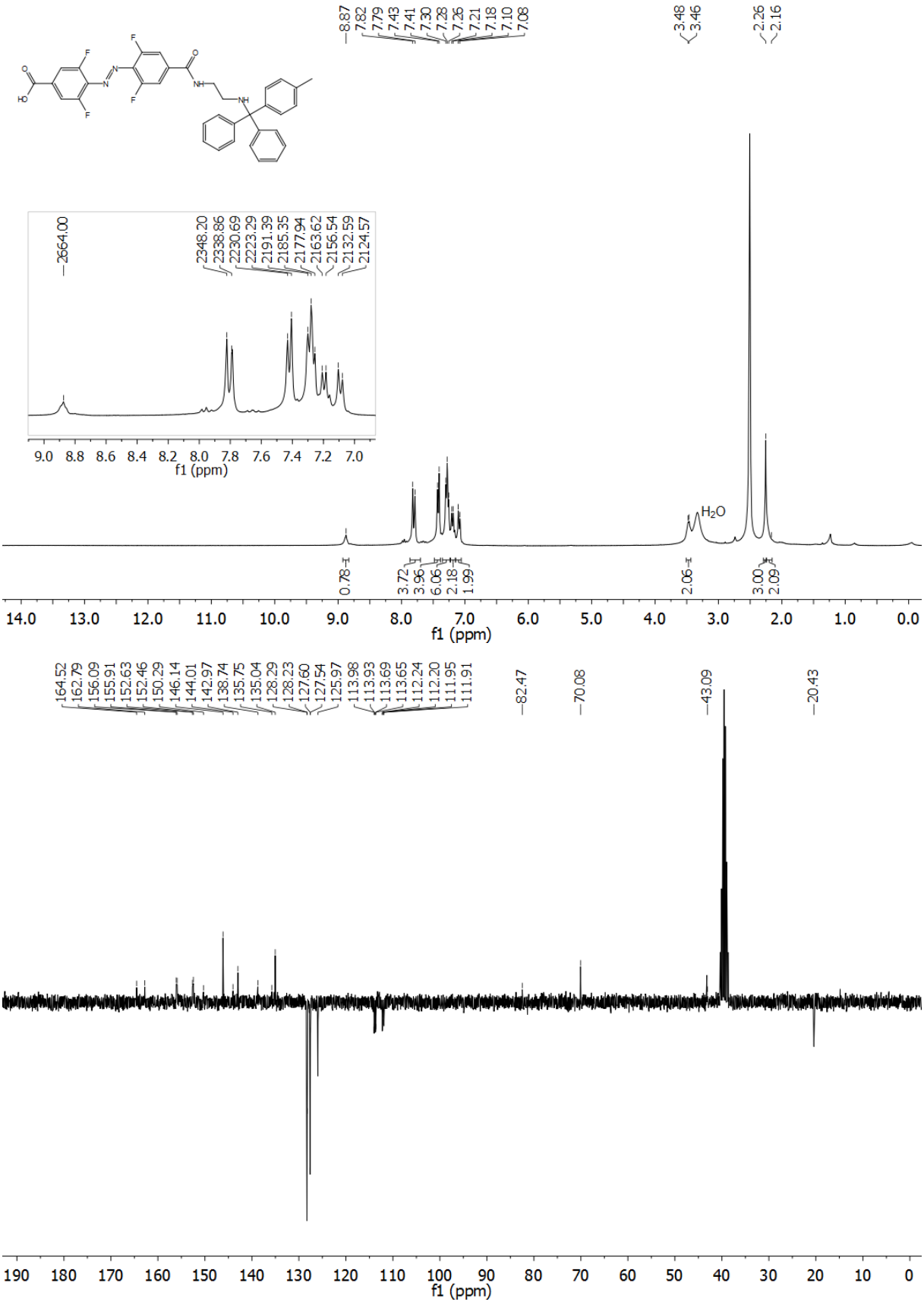

Figure S4. Top: ^{1}H-NMR spectrum of the compound **2**. Insert: zoom-in of signals in the aromatic region to highlight the shifts in Hz units for calculating *J*-constants. Bottom: ^{13}C-APT-NMR spectrum of compound **2**.

N1-(diphenyl(p-tolyl)methyl)ethane-1,2-diamine (**10**)

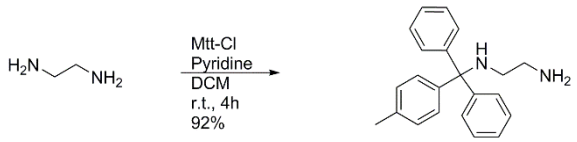

Following the procedure of Chouiki et al.[8] ethylene diamine (6.20 mL, 92.2 mmol, 9.00 eq) was dissolved in DCM (20.0 mL) and pyridine (14.4 mL) was added portionwise. Methyltrityl chloride (3.00 g, 10.25 mmol, 1.00 eq) was added at 0°C. The solution was stirred 4 h at r.t., before it was quenched by adding MeOH (5.50 mL) and the solvent was evaporated. The crude was dissolved in DCM (1% NEt_3)/ distilled water (1:1; 100 mL) and the product was extracted with DCM (2 x 50.0 mL). The combined organic layers were washed with brine, dried over anhydrous $MgSO_4$ and the solvent was removed under reduced pressure. The crude was purified by flash column chromatography (EtOAc + 3% NEt_3). The product **10** was obtained as a colourless oil (2.99 g, 9.45 mmol, 92%). The characterization is in agreement with the literature.[8] **TLC:** R_f = 0.2 (EtOAc + 3% Net_3) **^{1}H NMR (300 MHz, $CDCl_3$, δ):** 7.48 (dd, ^3J = 5.3 Hz, 4H, 4 × CH_{ar}), 7.35 (d, ^3J = 8.2 Hz, 2H, 2 × CH_{ar}), 7.30 – 7.22 (m, 4H, 4 × CH_{ar}), 7.21 – 7.12 (m, 2H, 2 × CH_{ar}), 7.07 (d, ^3J = 8.1 Hz, 2H, 2 × CH_{ar}), 2.79 (t, ^3J = 5.9 Hz, 2H, CH_2), 2.30 (s, 3H, CH_3), 2.20 (t, ^3J = 6.0 Hz, 2H, CH_2), 1.42 (s, 2H, NH_2). **^{13}C NMR (75 MHz, $CDCl_3$, δ):** 146.5 (2 × C_{ar}), 143.4 (C_{ar}), 135.87 (C_{ar}), 128.8 (4 × CH_{ar}), 128.7 (2 × CH_{ar}), 128.6 (4 × CH_{ar}), 127.9 (2 × CH_{ar}), 126.3 (2 × CH_{ar}), 70.6 (CNH), 46.7 (CH_2), 43.0 (CH_2), 21.1 (CH_3). **HRMS-ESI$^+$ (m/z):** calcd. for $[M + H]^+$ $C_{22}H_{24}N_2H$: 317.2021; found: 317.2011.

Solid Phase Peptide Synthesis

Peptides were synthesized manually in 2 mL polypropylen reactors with plunger and frit, (pore size 25 µm, Multi Syn Tech GmbH, Germany; for bigger scales, 15 mL reactors were used). TentaGel S RAM resin (0.25 mmol/g), Cl-Trt resin (1.0-1.8 mmol/g) or Sieber-amide resin (0.3-0.6 mmol/g), where the loading of the first amino acid for both Sieber-amide and Cl-Trt resin was determined, were used for synthesis.

Determination of the resin loading: The Fmoc group of a weighted amount of resin (~5.00 mg), previously loaded with the first amino acid was deprotected by adding twice a solution of 20% piperidine in DMF for 5 min (500 µL). The filtrates were collected and the absorbance was measured at 300 nm (ε_{300} (Fmoc) = 7800 M^{-1} cm^{-1})[9] on a TECAN 20M Spark plate reader and the loading was calculated. Loading of the resins was done as follows:

Sieber-amide resin: 2.00 eq. Fmoc-amino acid, 2.00 eq. OxymaPure (0.5 M in DMF), 2.00 eq. DIC were added to the resin for 45 min with a final concentration of 0.4 M of the amino acid. After washing, the non-reacted amino groups were capped following the general protocol of manual synthesis explained below

Cl-Trt resin: 2.00 eq. Fmoc-amino acid, 8.00 eq. DIPEA in DMF were added to the resin for 45 min with a final concentration of 0.4 M of the amino acid. The Cl-Trt resin was capped by washing with 3 × DMF, 3 × DCM, 3 × DMF, 3 × MeOH, 3 × DCM.

Manual Solid Phase Protocol for Peptide Synthesis

The amounts of reagents of the following synthesis protocol correspond to 20-40 µmol scale. For higher scales, the reagents were scaled up correspondingly. For shaking an Edmund Bühler Swip shaker was used.

Swelling: The appropriate amount of resin was swollen in 1.0 mL DMF for 30 min.

Deprotection of the temporal Fmoc group: Piperidine (500 µL, 20% in DMF) was added to the resin and was shaken for 5 min. This step was repeated and the resin was filtered off and washed with DMF (5 × 1.50 mL), CH_2Cl_2 (5 × 1.50 mL), DMF (5 × 1.50 mL).

Coupling of amino acids: The Fmoc-amino acid (4.00 eq.) was dissolved in OxymaPure (0.5 M in DMF, except for the coupling of the the azobenzene derivatives, where OxymaPure was dissolved in NMP, 0.5 M, 4.00 eq.), and DIC (4.00 eq.) was added. The resulting solution was activated for 3 min and subsequently added to the resin. This suspension was shaken for 45 min. The resin was filtered off and washed with DMF (5 × 1.50 mL) and CH_2Cl_2 (5 × 1.50 mL) and DMF (5 × 1.50 mL). Monitoring of the coupling completion was confirmed by the TNBS-test[10] on few resin-beads.

Capping: A solution of lutidine/Ac_2O/DMF 6:5:89 (1.0 mL) was added to the resin and was shaken for 5 min. The resin was filtered off and washed with DMF (5 × 1.50 mL), CH_2Cl_2 (5 × 1.50 mL) and DMF (5 × 1.50 mL).

Cleavage deprotection step: Depending on the specific peptide the cleavage cocktail differed in the concentration of TFA or HFIP, type of scavengers and reaction times. The used cleavage cocktails and reaction times are listed below.

- Cleavage cocktail A: 95% TFA, 5% H_2O (2 h)

- Cleavage cocktail B: HFIP/CH_2Cl_2 1:4 (3 h)

- Cleavage cocktail C: 1% TFA in CH_2Cl_2 (2 × 30 min)

- Cleavage cocktail D: 90% TFA, 10% H_2O (90 min)

The dried resin was treated with the corresponding mixture and was shaken for the specific time. After the defined time, the resin was filtered off and the filtrate was added to dry ice-cold Et_2O (1 mL of Et_2O for 100 µL cleavage cocktail). After 10 min, the precipitated peptide was centrifuged, the supernatant was discarded and the peptide pellet was dissolved in MilliQ in order to be purified.

Purification: The probes were purified as specified above. The collected fractions, containing the desired peptides, were lyophilized and stored at -20 °C.

Characterization: The freeze-dried products were identified via analytical HPLC-MS on an Agilent 1200 Series HPLC-system (Agilent Technologies) as detailed before. Electrospray Ionization Mass Spectrometry (ESI-MS) was performed as detailed before.

Synthesis and Characterization Data of the Peptides

Unless otherwise noted, the synthesis of the peptides was performed manually following the protocol described above. The purity of the peptides was calculated from the integrated peak areas of the HPLC chromatograms, and is given as % for each peptide. In the chromatograms, the different isomers of azobenzene-containing peptides are labelled with their respective retention times above the respective peak and assigned in the text into brackets.

4: H_2N-Ser-Ala-Arg-Ala-**cAzo**-Val-His-Leu-Arg-Lys-Ser-$CONH_2$; For the final cleavage step, the resin (scale = 20 µmol, loading = 0.25 mmol/g) was treated with 2.00 mL cleavage cocktail A. After purification, the product 5 × TFA salt (3.8 mg, 1.83 µmol, 9%) was obtained as a yellow solid. t_R = 23.36 min (*cis*). Purity ≥ 99%. Formula: $C_{63}H_{100}N_{24}O_{13.}$ HRMS-ESI$^+$ (m/z): $[M+2H]^{2+}$ calcd.: 701.4026; found: 701.4028.

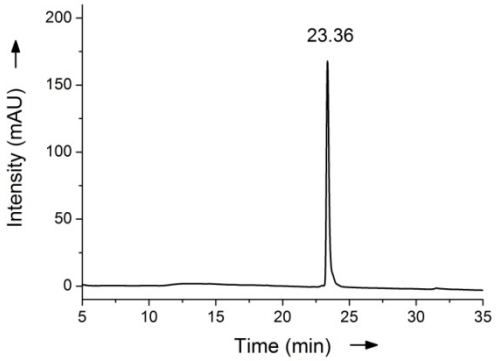

Figure S5. HPLC chromatogram of purified peptide **4**. Gradient: 5-40% B on column 1.

16: Boc-Ser(tBu)-Ala-Arg$(Boc)_2$-Ala-COOH; For the final cleavage step, the resin (scale = 0.35 mmol, loading = 0.832 mmol/g) was treated with 14.00 mL cleavage cocktail B. After purification, the product (146.5 mg, 0.193 mmol, 55%) was obtained as a white solid. t_R = 24.09 min. Purity = 99%. Formula: $C_{34}H_{61}N_7O_{12.}$ HRMS-ESI$^+$ (m/z): $[M+H]^+$ calcd.: 760.4451; found: 760.4445.

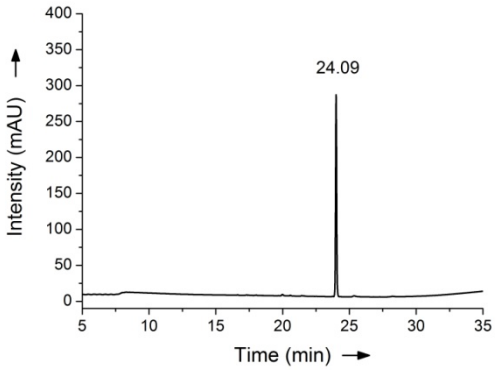

Figure S6. HPLC chromatogram of purified peptide **16**. Gradient: 5-95% B on column 1.

17: H_2N-***o*F$_4$Azo**-Val-His(Trt)-Leu-Arg(Boc)$_2$-Lys(Boc)-Ser(tBu)-$CONH_2$; For the final cleavage step, the resin (scale = 80 µmol, loading = 0.513 mmol/g) was treated with 6.00 mL cleavage cocktail C, 2 × for 30 min. After purification, the product 1 × TFA-salt (33.9 mg, 18.7 µmol, 23%) was obtained as an orange solid. t_R = 14.95 min (*cis*, product - 1Boc), 15.70 min (*trans*, product - 1Boc), 19.55 min (*cis*), 20.39 min (*trans*). Purity = 91%. Formula: $C_{86}H_{116}F_4N_{17}O_{15}$. HRMS-ESI$^+$ (m/z): $[M+H]^+$ calcd.: 1703.8798; found: 1703.8778.

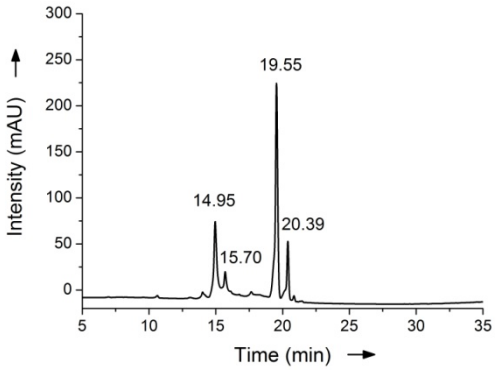

Figure S7. HPLC chromatogram of purified peptide **17**. Gradient: 35-95% B on column 2.

*Ligation of fragments **16** and **17***

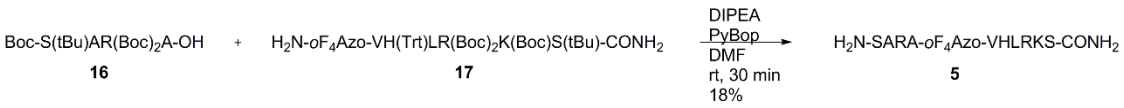

Scheme S10. Ligation of fragments **16** and **17** to form final ***o*F$_4$Azo-peptide 5**.

5: H_2N-Ser-Ala-Arg-Ala-***o*F$_4$Azo**-Val-His-Leu-Arg-Lys-Ser-$CONH_2$; Ligation of the two fragments **16** and **17** was performed in solution. Therefore, **17** (33.9 mg, 0.0187 mmol, 1.00 eq.) was dissolved in 187 µL DMF and DIPEA (3.30 µL, 0.0187 mmol, 1.00 eq) was added. Peptide **17** (42.6 mg, 0.056 mmol, 3.00 eq.) was separately, dissolved in 187 µL DMF, where PyBop (29.1 mg, 0.056 mmol, 3.00 eq.) and DIPEA (26.1 µL, 0.15 mmol, 8.00 eq) were added and the mixture was activated for 3 min before it was added to the solution of **17**. The reaction mixture was shaken for 30 min. After purification, the side chain protecting groups were deprotected by treatment of the crude with 20 mL cleavage cocktail D. The product was precipitated in ice cold Et_2O, dissolved in water and irradiated at 520 nm as explained before to obtain the *cis* isomer, which was isolated via preparative HPLC. The product 5 × TFA-salt (6.9 mg, 3.35 µmol, 18%) was obtained as an orange solid. t_R = 21.74 min (*cis*), 22.25 min (*trans*). Purity = 99%. Formula: $C_{63}H_{98}F_4N_{24}O_{14}$. HRMS-ESI$^+$ (m/z): $[M+2H]^{2+}$ calcd.: 745.3810; found: 745.3804.

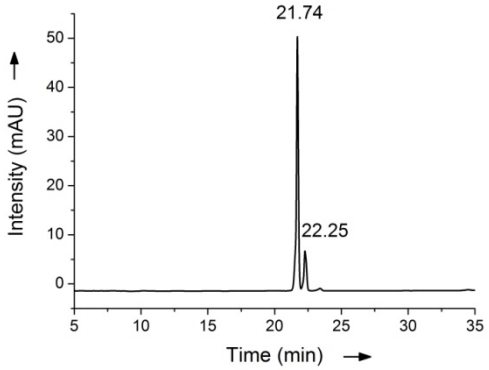

Figure S8. HPLC chromatogram of purified peptide **5**. Gradient: 5-40% B on column 2.

Results and Discussion

Screening for Suitable Fmoc-deprotection Conditions

To test whether the *o*F_4Azo motif could be introduced into the peptide backbone as an Fmoc-amino acid building block, first the stability of the compound **9** against 5% piperazine in DMF and 2% DBU in DMF was evaluated since these conditions could be used as mild protocol for Fmoc-deprotection in SPPS.

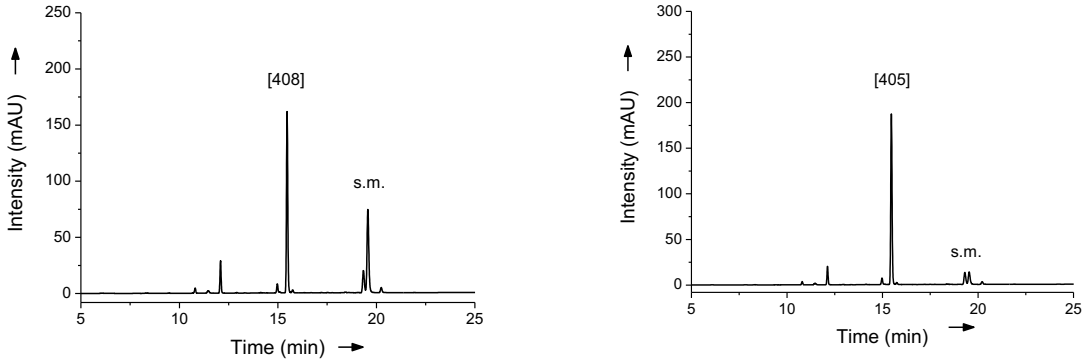

Figure S9. HPLC chromatograms of *o*F_4Azo compound **5**. Gradient 5-95% B on column 2. Left: 5% piperazine in DMF, 10 min. Right: 2% DBU in DMF, 10 min. Mass of degradation products indicated on top of the peak in square brackets and g/mol.

As obvious from the HPLC chromatograms these conditions are not compatible with the stability of **9**, since they lead to adduct formation as side products in the case of the piperazine and substitution side products in the case of DBU.

To further evaluate this, we incorporated the **Mtt-*o*F_4AzoAA 2** to the peptide backbone of the VHLRKS-peptide fragment via the general SPPS method detailed before. As shown in Scheme S11, the Mtt-protecting group was removed on the resin via washing the resin with 1% TFA in DCM (10 × 1 min) followed by the washing with DCM, DMF, MeOH, DMF, DCM and DMF (each 3 × 1 min). Then, the resin was again washed with 20% DIPEA in DMF (5 × 3 min), before Fmoc-Ala-OH was coupled according to the usual SPPS protocol.

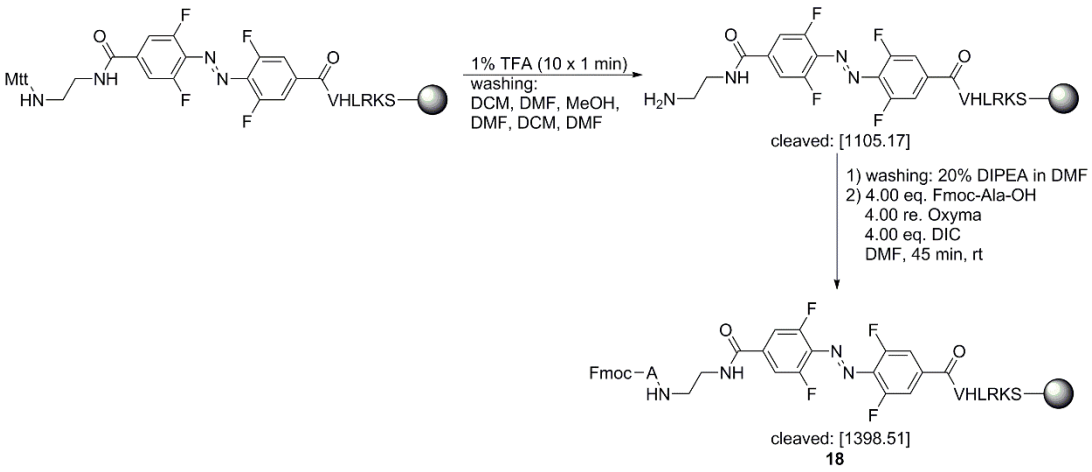

Scheme S11. On resin Mtt-deprotection and coupling of Fmoc-Ala-OH to the *o*F_4Azo-peptide fragment.

The HPLC chromatogram and the ESI spectrum of the cleaved compound **18** are shown in Figure S10 (19.12 and 19.89 min: *cis* and *trans* isomer of **18**, respectively).

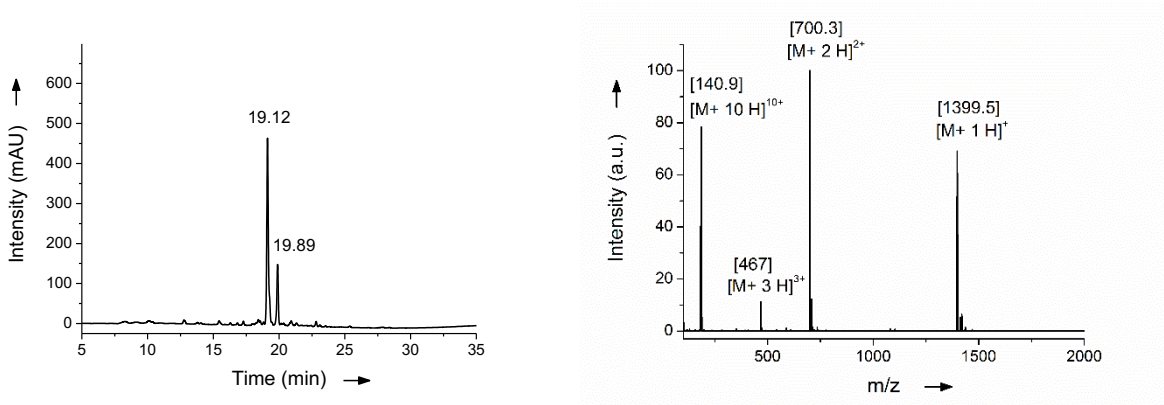

Figure S10.. Left: HPLC chromatogram of Fmoc-protected product **18** with a mass of 1398.51 g/mol. Gradient 5-95% B, column 2. Right: ESI spectrum of compound **18**.

The resin was then incubated with the respective Fmoc-deprotection conditions (see Scheme S12 and Table 1, Manuscript) and then washed and dried as in the general SPPS protocol. Next, a test cleavage with the cocktail D (90% TFA, 10% H_2O, 90 min) was performed and HPLC chromatograms were recorded (5-95% B, column 2), which are shown in Figure S11 till Figure S13.

Scheme S12. Reaction for the evaluation of different Fmoc-deprotection conditions on the peptide fragment **18**.

The peaks at 19.12 and 19.89 min correspond to the Fmoc-protected peptide **18** with a mass of 1398.51 g/mol. The peak at 14.25 min corresponds to the desired Fmoc-deprotected product **19** with a mass of 1176.2 g/mol. The masses of the additional new peaks are indicated in square brackets in g/mol above the respective peak.

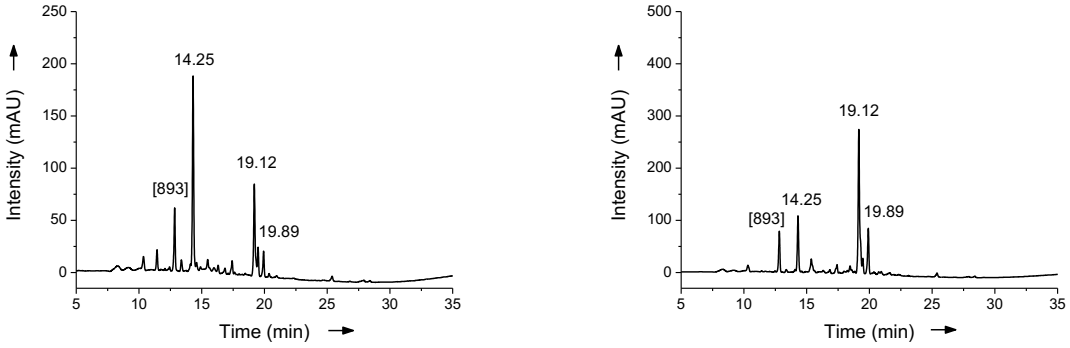

Figure S11. HPLC chromatograms after Fmoc-deprotection and resin cleavage with cocktail D. Gradients 5-95% B, column 2. Left: Conditions A incubated for 17 h. Right: Conditions B incubated for 17 h.

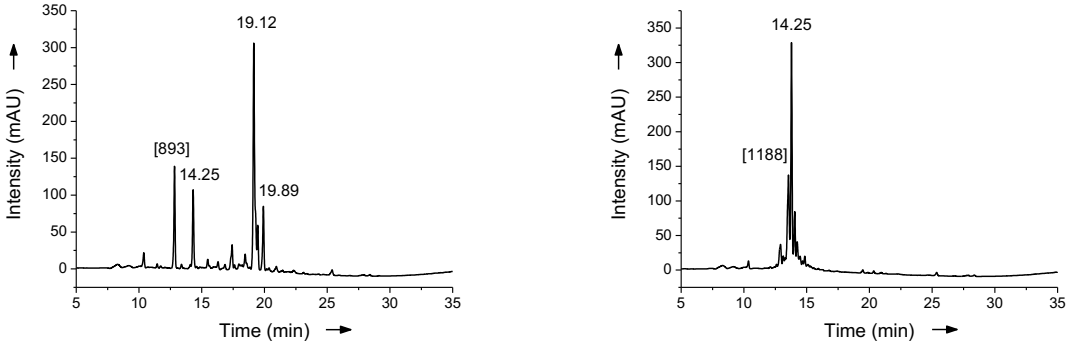

Figure S12. HPLC chromatograms after Fmoc-deprotection and resin cleavage with cocktail D. Gradient 5-95% B, column 2. Left: Conditions C incubated for 17 h. Right: Conditions D incubated for 90 min.

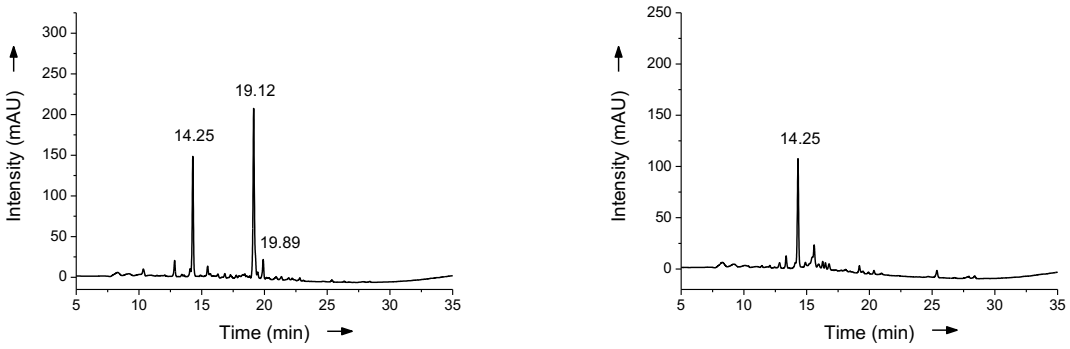

Figure S13. HPLC chromatograms after Fmoc-deprotection and resin cleavage with cocktail D. Gradient 5-95% B, column 2. Left: Conditions E incubated for 3 h. Right: Conditions F incubated for 16 h.

As can be seen, almost none of the above detailed conditions could prove to be efficient for Fmoc deprotection without the degradation of the peptide (A, B, C, D). The only exception is

condition E/F, with which it was possible to deprotect the Fmoc group without a notably high degradation of the peptide.

Extinction Coefficients

The extinction coefficient of cAzo-containing peptide **4**, was measured in MilliQ water at r.t. A specific amount of the compound **4** (> 5.00 mg) was accurately weighted on a Mettler Toledo XP6 micro balance to prepare a solution of known concentration. Increasing amounts of the corresponding stock solution were added without exceeding 10 % of the initial volume of the cuvette; absorbance was measured as explained before. In all the cases the recorded absorbance was between 0.1 and 1 a.u. to be in concordance with Lambert-Beer law:

$A = \varepsilon \cdot c \cdot l$

where A = absorbance; ε = molar extinction coefficient; c = concentration; l = path length.

The lineal regression of the obtained absorbance measurements versus the concentrations of the corresponding compound allowed us to obtain the molar extinction coefficient and regression value (R^2). The background signal was subtracted.

The obtained molar extinction coefficient in MilliQ water is: $\mathcal{E}_{494}$ = 25990 L mol^{-1} cm^{-1} with R^2 = 0.995

In the case of the other peptides the following extinction coefficients were used: *o*F$_4$Azo containing peptides (for *trans* isomer) $\mathcal{E}_{319}$ = 25000 L mol^{-1} cm^{-1} in MeCN,[1] cAzo containing peptides (for *cis* isomer) $\mathcal{E}_{238}$ = 25990 L mol^{-1} cm^{-1} in MilliQ water, fluorescently tagged peptides $\mathcal{E}_{494}$ = 76900 L mol^{-1} cm^{-1}[2] in 0.1 M phosphate buffer, pH = 9).

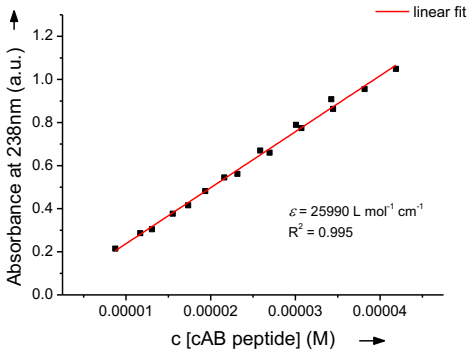

Figure S14. Linear fit of the triplicate measurements to obtain the extinction coefficient of cAzo-containing peptide **4**.

UV-vis Characterization

For the characterization via UV-vis measurements of the *o*F$_4$Azo-containing peptide **5** and cAzo containing peptide **4**, a Tecan (Switzerland) Spark 20M multimode microplate reader was used. 200 µL of a 0.262 mM solution of *o*F$_4$Azo-containing peptide **5** in MilliQ water was added to a blank of 300 µL MilliQ water in a cuvette (final conc.: 0.105 mM). The cuvette was irradiated at the respective wavelengths for the indicated times, followed by measuring the absorbance spectra at r.t. To evaluate the required time of irradiation to reach the photostationary state

(PSS) of one isomer, the two isomers were irradiated for different times. The absorbance spectra are shown in Figure S15.

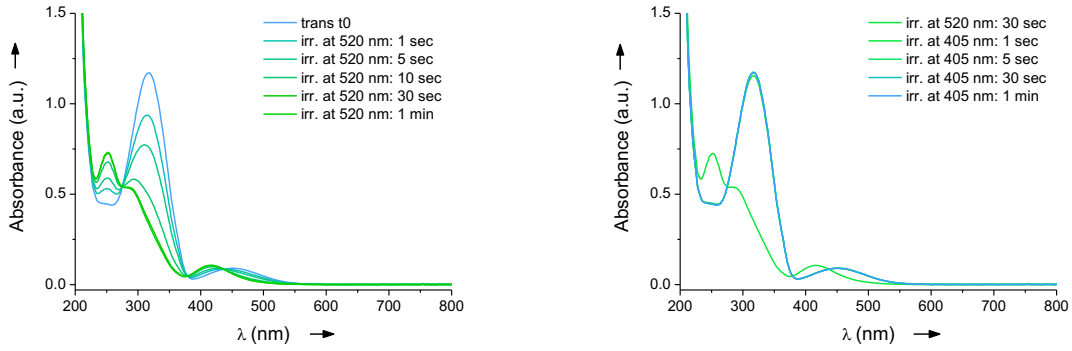

Figure S15. UV-vis spectra of *o*F_4Azo-containing peptide **5**. Left: irradiation of *trans* isomer at 520 nm to obtain the *cis* isomer. Right: irradiation of *cis* isomer at 405 nm to obtain the *trans* isomer.

For the characterization via UV-vis measurements of the cAzo-containg peptide **4**, 100 µL of a 0.51 mM solution of cAzo-containg peptide **4** in MilliQ water was added to a blank of 300 µL water in a cuvette (final conc.: 0.128 mM). The procedure was the same as detailed above. The absorbance spectra are shown in Figure S16.

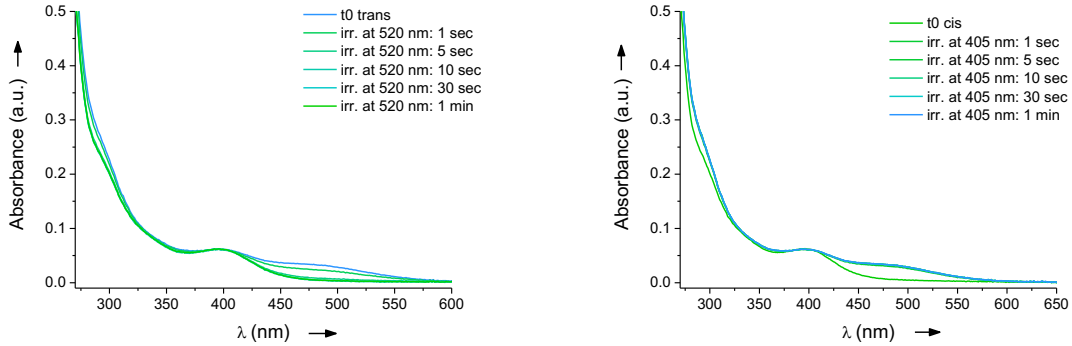

Figure S16. UV-vis spectra of cAzo-containg peptide **4**. Left: irradiation of *trans* isomer at 520 nm to obtain the *cis* isomer. Right: irradiation of *cis* isomer at 405 nm to obtain the *trans* isomer.

RP-HPLC Characterization

In the case of the *o*F_4Azo-containing peptide **5** the *trans* isomer is the thermodynamically more stable one. Contrarily for the cAzo-containing peptide **4**, the *cis* isomer is thermodynamically favoured due to the ring strain of the *trans* isomer. To evaluate the ratio of each isomer at their photostationary states, as well as examining the stability of each isomer in total darkness, we used RP-HPLC, if not stated differently, the column 3 and a gradient of 10-35% B for *o*F_4Azo-containing peptide **5** and 5-40% B for cAzo-containing peptide **4** were used.

For the isomerization, a 120 µM solution of the corresponding peptide in MilliQ water was irradiated at 405 nm for 5 sec to obtain the *trans* isomer, and at 520 nm for 1 min to obtain the *cis* isomer for the *o*F_4Azo-containg peptide **5.** For the cAzo-containing peptide **4**, at 405 nm for 1 min to obtain the *trans* isomer, and at 520 nm for 10 sec. to obtain the *cis* isomer. The

photostationary states reached upon irradiation were determined by integrating the peak areas in the HPLC chromatograms at 275 nm (*o*F$_4$Azo- containing peptide **5**, isosbestic point) and at 395 nm (cAzo-containing peptide **4**); due to the low ratio of the *trans* isomer in its photostationary state, the isosbestic point is not clearly visible in these spectra. Because of this, the *cis*/*trans* ratio of peptide **4** was determined via HPLC at 395 nm, which is the wavelength where both isomers show the same height of absorbance and have, therefore, the same extinction coefficient). To evaluate the relaxation times, the peptide solutions were stored in total darkness at r.t. and HPLC chromatograms were recorded after the indicated time periods, shown in Figure S17 for the *o*F$_4$Azo-containing peptide **5** and in Figure S18 for the cAzo-containing peptide **4**.

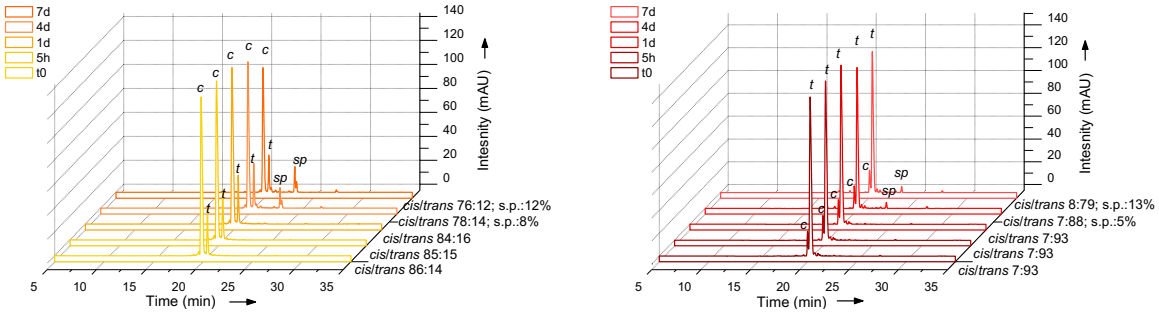

Figure S17. HPLC chromatograms of *o*F$_4$Azo-containg peptide **5** incubated in total darkness. HPLC chromatograms were recorded after the indicated time. c: *cis*, t: *trans*, sp: side product. Left: after irradiation at 520 nm to reach the photostationary state of the *cis* isomer. Right: after irradiation at 405 nm to reach the photostationary state of the *trans* isomer. s.p.: indication of ratio of side products.

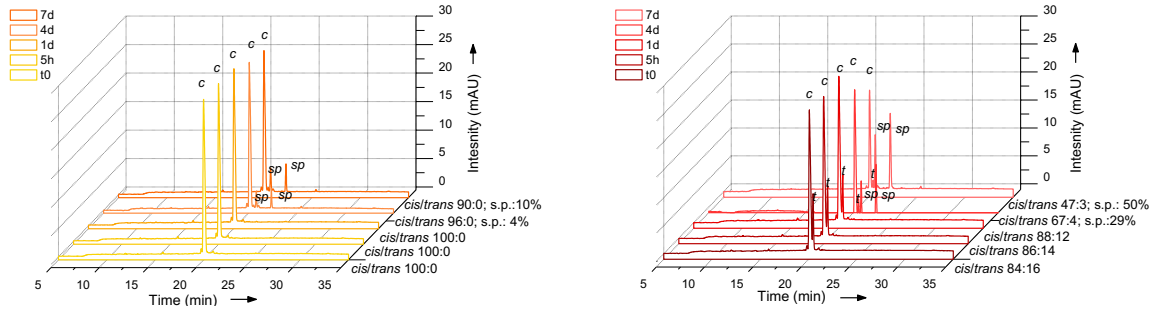

Figure S18. HPLC chromatograms of cAzo-containg peptide **4** incubated in total darkness. HPLC chromatograms were recorded after the indicated time. c: *cis*, t: *trans*, sp: side product. Left: no irradiation; photostationary state of the *cis* isomer. Right: after irradiation at 405 nm to reach the photostationary state of the *trans* isomer. s.p.: indication of ratio of side products.

NMR Characterization

To confirm the ratio between isomers of the oF$_4$Azo-containing peptide **5**, obtained by HPLC characterization, we used 1H-NMR. The NMR spectra of peptides **5** was recorded in D_2O at 300 K a Bruker AV III HD 600 MHz at a frequency of 600 MHz (^{1}H), as detailed above. The peptide was dissolved in D_2O to give a solution of 1.34 mM concentration. Then, the solution was irradiated at the corresponding wavelength as detailed above and 1H-NMRs of each isomer were recorded. The aromatic region of the spectra are shown in Figure S19. The *cis*/*trans* ratios were calculated by integrating the peak areas of these aromatic proton signals, (**5**: irr. at 405 nm: *cis*/*trans*: 8:92; at 520 nm: 84:16 by NMR) and they corroborate the HPLC

ratios. Of note, under our conditions neither the amide protons[11–13] nor the aromatic histidine protons[14,15] were visible.

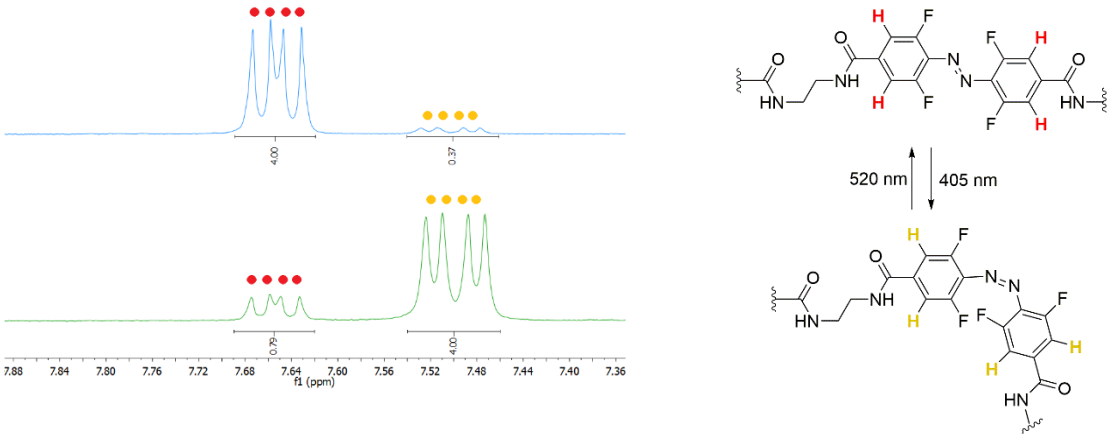

Figure S19. Selected aromatic region of the 1H-NMR spectra (600 MHz) of a1.34 mM solution of ***o*F$_4$Azo-peptide** (**5**) in D_2O after irradiation to the *trans*- (top, blue) and *cis* (bottom, green) isomer. Aromatic protons are marked in colours on the spectra and molecules.

Stability against Glutathione

The stability of the peptides **5** and **4** against glutathione (GSH) was evaluated by incubating 3.5 µL of a 250 mM stock of GSH with 80 µL of a 100 µM solution of the respective peptide in MilliQ water giving final concentrations of 10 mM of GSH and 96 µM of the peptides, respectively at r.t. After different time periods, HPLC chromatograms of these mixtures were recorded and are shown in Figure S20 to Figure S21 (column 3, gradient of 10-35% B for *o*F$_4$Azo-containing peptide **5** and 5-40% B for cAzo-containing peptide **4**).

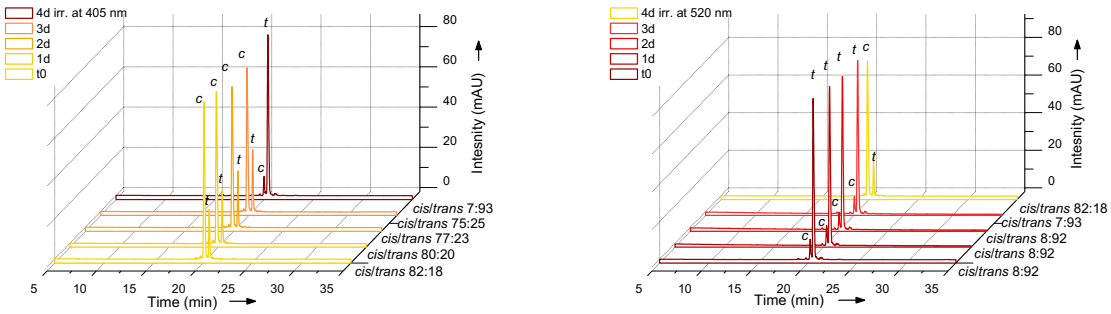

Figure S20. HPLC chromatograms of *o*F$_4$Azo-peptide (**5)** incubated with 10 mM reduced glutathione at 275 nm. The solutions were stored in darkness and HPLC chromatograms were recorded after the indicated time. c: *cis*, t: *trans*, sp: side product. Left: after irradiation at 520 nm to reach the photostationary state of the *cis* isomer. After 4 days incubation, the solution was irradiated at 405 nm to switch back to the photostationary state of the *trans* isomer (red). Right: after irradiation at 405 nm to reach the photostationary state of the *trans* isomer. After 4 days incubation, the solution was irradiated at 520nm to switch back to the photostationary state of the *cis* isomer (yellow).

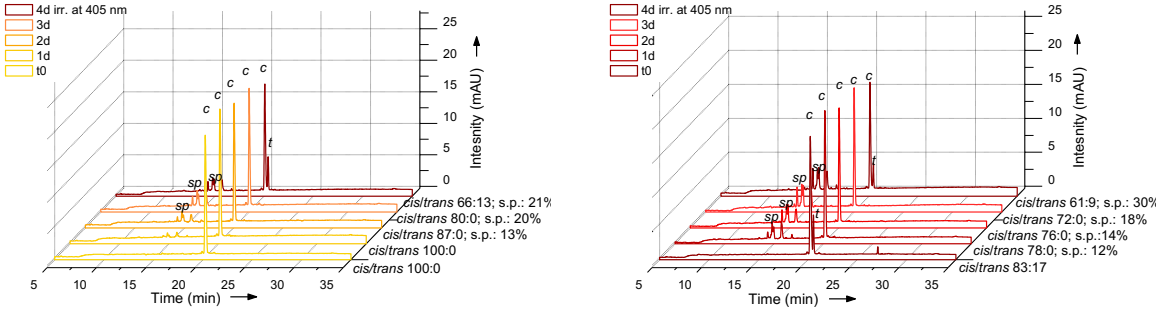

Figure S21. HPLC chromatograms of **cAzo-peptide** (**4**) incubated with 10 mM reduced glutathione. The solutions were stored in darkness and HPLC chromatograms were recorded after the indicated time. c: *cis*, t: *trans*, sp: side product. Left: after irradiation at 520 nm to reach the photostationary state of the *cis* isomer. After 4 days incubation, the solution was irradiated at 405 nm to switch back to the photostationary state of the *trans* isomer (red). Right: after irradiation at 405 nm to reach the photostationary state of the *trans* isomer. After 4 days incubation, the solution was again irradiated at 405 nm to switch back to the photostationary state of the *trans* isomer (red). s.p.: indication of ratio of side products.

Fluorescence Polarization-based Assay

Competitive Fluorescence Polarization-based Binding Assays

The FP-binding experiments were performed in triplicate and three times independently. The results are represented in Table S1 and the FP spectra are shown in Figure 2 (Manuscript).

Table S1. Mean ± SD of the IC_{50} and K_i values of peptides **4** and **5** of three independent measurements.

peptide	Exp.	PSS at 405 nm IC_{50} [µM]	PSS at 520 nm IC_{50} [µM]	PSS at 405 nm K_i [µM]	PSS at 520 nm K_i [µM]	ratio
H_2N-SARA**oF$_4$Azo**VHLRKS (**5**)	1	0.757	1.88	10.9	28.7	2.63
	2	0.759	1.91	11.0	29.1	2.65
	3	0.913	2.27	13.4	34.7	2.59
	mean	0.810 ± 0.089	2.02 ± 0.21	0.0118 ± 0.0014	0.0308 ± 0.0033	2.61
H_2N-SARA**cAzo**VHLRKS (**4**)	1	7.07	9.58	0.110	0.150	1.36
	2	8.53	16.1	0.133	0.252	1.89
	3	11.4	14.0	0.178	0.220	1.24
	mean	8.98 ± 2.18	13.2 ± 3.3	0.140 ± 0.035	0.207 ± 0.052	1.48

To verify that the used assay conditions do not influence the *cis*/*trans* ratio, a control well with 5 µL of the respective peptide in DMSO irradiated at 525 nm (*cis*), as well at 405 nm (*trans*), each diluted with 120 µL assay buffer were included in each plate. Before and after the assay, HPLC chromatograms of such controls were recorded at the respective isosbestic points (gradient: 5-40% B, column 2). We did not observe any influence on *cis*/*trans* ratio due to the assay conditions. The chromatograms are shown in Figure S22 to Figure S25. *Cis* and *trans*

isomers are labelled with their respective retention times (**5**, *cis*: 20.07/19.91 min; **5**, *trans*: 20.40/20.49 min; **4**, *cis*: 20.02 min; **4**, *trans*: 20.42 min).

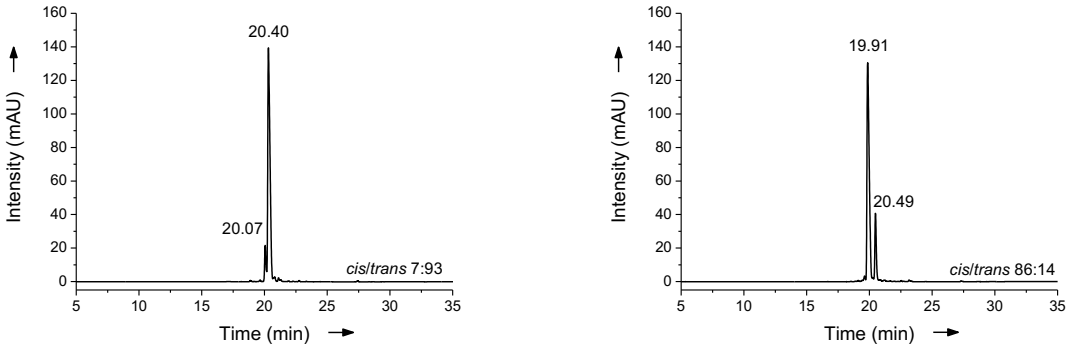

Figure S22. HPLC chromatograms of peptide **5** (SARA-***o*F$_4$Azo**-VHLRKS) before the FP-based assay. Left: irradiated peptide at 405 nm. Right: irradiated peptide at 520 nm.

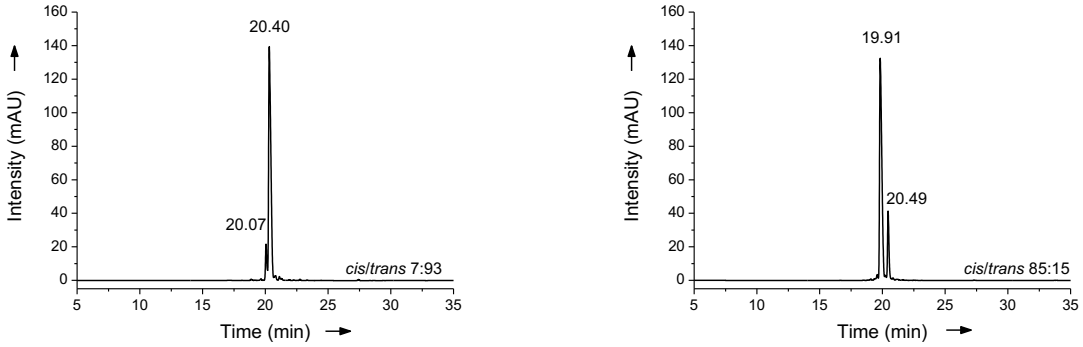

Figure S23. HPLC chromatograms of peptide **5** (SARA-***o*F$_4$Azo**-VHLRKS) after the FP-based assay. Left: irradiated peptide at 405 nm. Right: irradiated peptide at 520 nm.

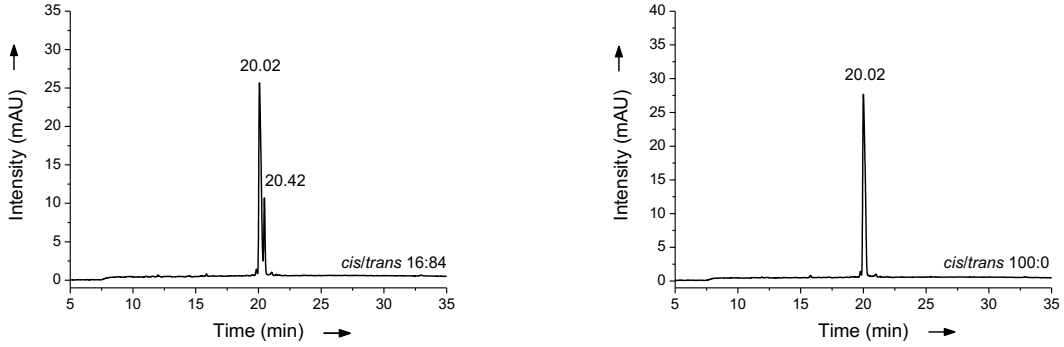

Figure S24. HPLC chromatograms of peptide **4** (SARA-**cAzo**-VHLRKS) before the FP-based assay. Left: irradiated peptide at 405 nm. Right: irradiated peptide at 520 nm.

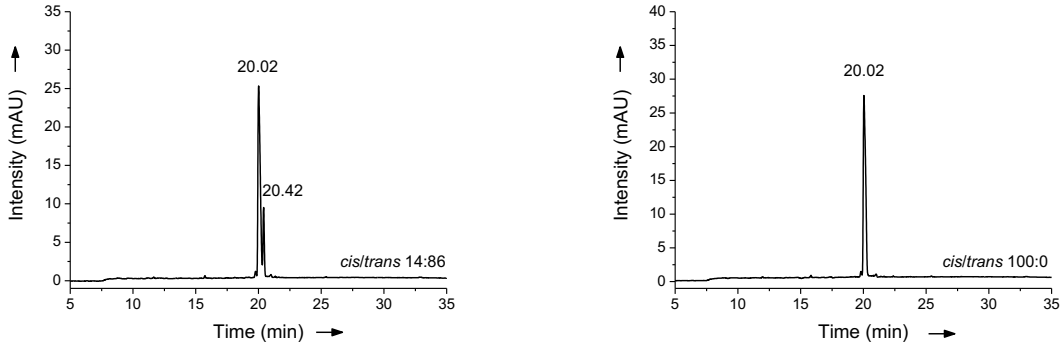

Figure S25. HPLC chromatograms of peptide **4** (SARA-**cAzo**-VHLRKS) after the FP-based assay. Left: irradiated peptide at 405 nm. Right: irradiated peptide at 520 nm.

Crystallisation of WDR5Δ23-Peptide 4 Complex

Figure S26 shows an overlay of the whole structures of the superimposed **cAzo-peptide** (**4**) with **AMPB-peptide** (**3**), as well as the ribbon representation of **4** showing its helical conformation. Figure S27 represents the hydrogen bonds of peptide **4** to WDR5.

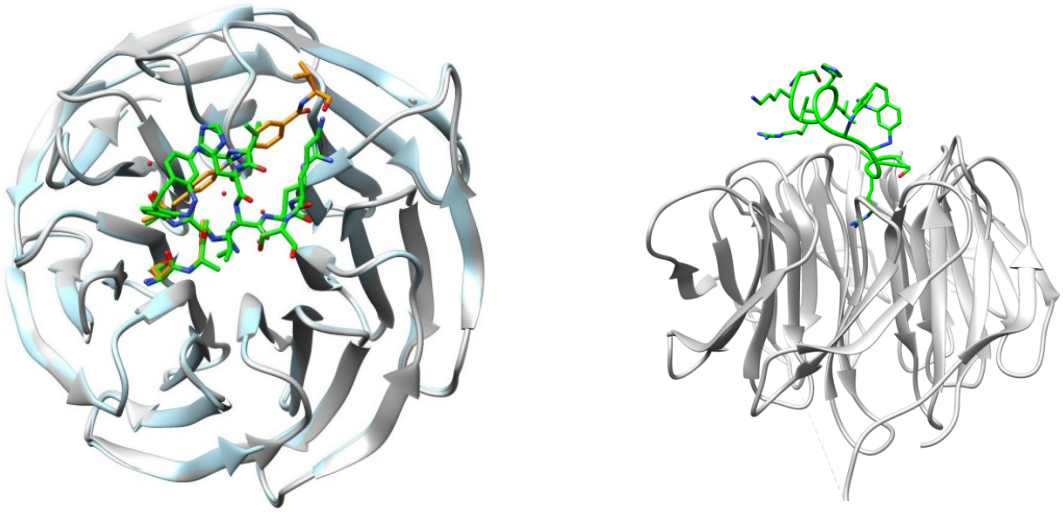

Figure S26. Right: Superposition of the crystal structure of the WDR5Δ23/cAzo peptide **4** and WDR5Δ23/AMPB-peptide (**3**) (peptide **3**: orange, peptide **4**: green). Left: Ribbon representation of cAzo-peptide (**4**) (green) showing its helical conformation.

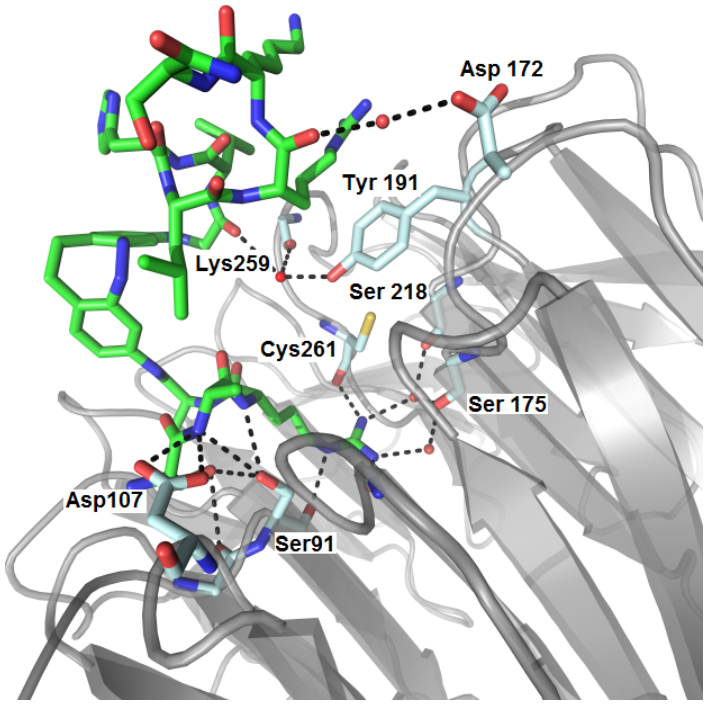

Figure S27. Hydrogen bond network of peptide **4** to WDR5Δ23 (peptide **4**: green). Interacting protein residues are labelled.

All the interactions between peptide **4** with WDR5Δ23 are shown in Figure S28 and are additionally listed in Table S2.

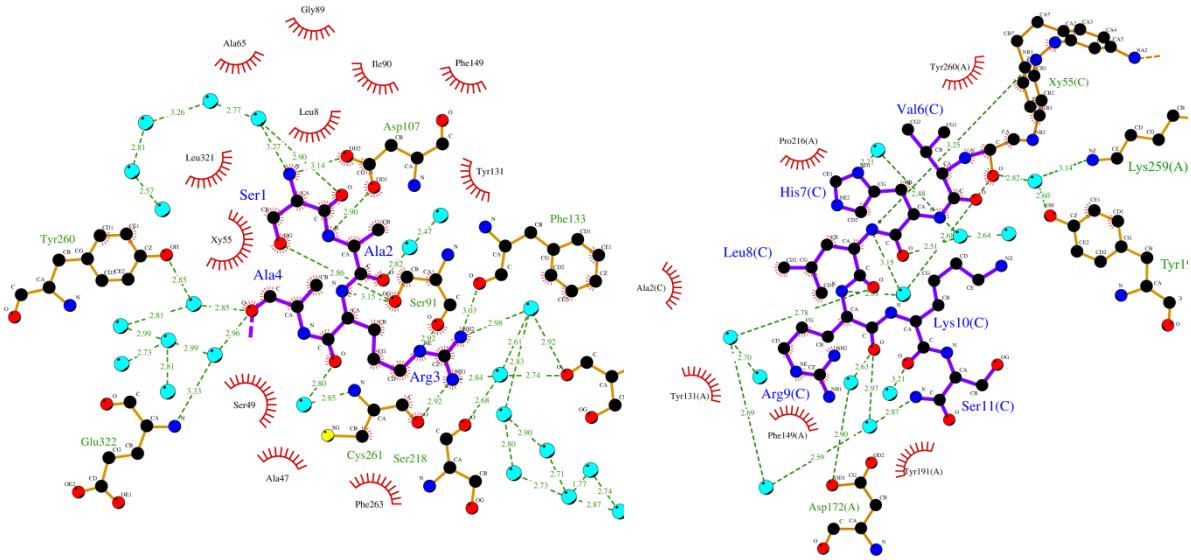

Figure S28. Schematic representation of the key interactions between the cAzo-peptide **4** and WDR5Δ23. Left: SARA part. Right: cAzo-VHLRKS part. Generated with LIGPLOT.[16]

Table S2. Interactions between the **cAzo-peptide** (**4**) and WDR5Δ23.

peptide		Hydrogen-bond/ Van der Waals partner		
Residue	Atom	WDR5 residue	Atom	Distance (Å)
Ser1	OG	Ser91	OG	2.86
Ser1	N	Asp107	OD2	3.14
Ala2	N	Asp107	OD1	2.90
Arg3	O	water (bridge to Cys261, N)	O	2.80
Arg3	NH1	Cys261 water (bridge to Ser175, O)	O O	2.92 2.84
Arg3	NH2	Phe133 water (bridge to Ser175, O and via another water to Ser218, O)	O O	3.03 2.98
Ala4	O	water (bridge to Tye260, O) water (bridge to Glu322, N)		2.85 2.96
cAzo	O	water (bridge to Tyr191, OH) water (bridge to lys259, NH2)		2.82
Arg9	O	Water (bridge to Asp172, OD1)	O	2.63

H-bond cut off < 3.5 Å, Van der Waals: 3.6-4.0 Å.

Docking and Molecular Dynamics (MD) Studies

The following Figures show the differences between poses obtained from molecular docking, molecular dynamics (MD) and the crystal structure of **AMPB-peptide** (**3**, PDB code: 5M23), as well as RMSD fluctuations during 20 ns of molecular dynamics, and fluctuations of residues from peptidomimetics during 20 ns of molecular dynamics simulations. Furthermore, the measured distances between leucine and tetra-*ortho*-fluorazobenzene, the difference in binding modes obtained for *cis* **AMPB-peptide** (**3**) and *cis* ***o*F$_4$Azo-peptide** (**5**) and the surface area of protein-peptidomimetics binding. Additionally, Figures that show the different binding modes of the **AMPB-peptide** (**3**) and the *cis*/*trans* ***o*F$_4$Azo-peptide** (**5**) obtained by MD, are represented, as well as the difference of computational predicted binding modes between *cis* and *trans* **cAzo-peptide** (**4**).

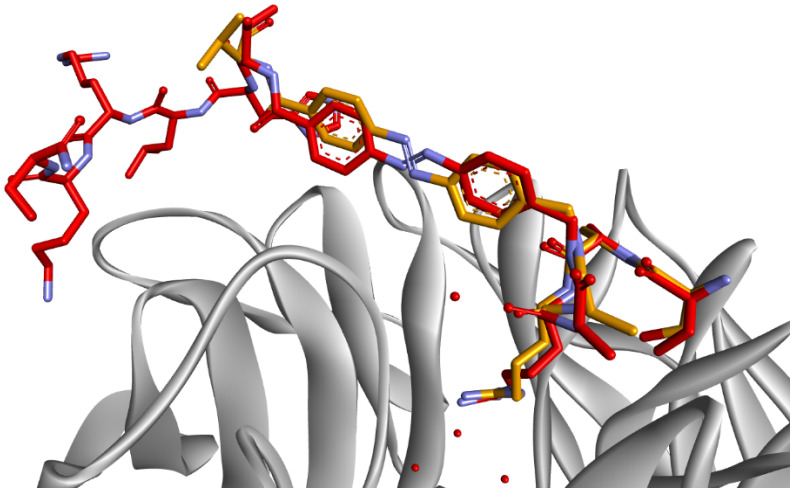

Figure S29. Difference between pose of *trans* **AMPB-peptide** (**3**) obtained by molecular docking (red sticks) and pose from PDB ID:5M23 (orange sticks).

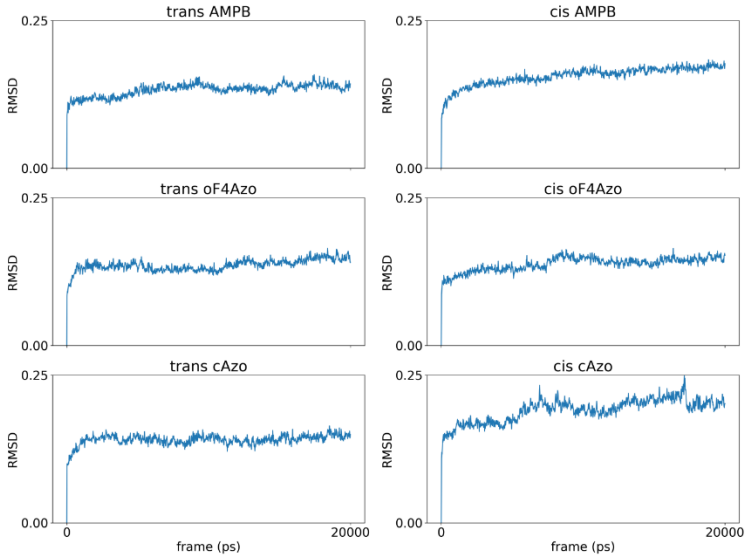

Figure S30. RMSD fluctuations during 20 ns of molecular dynamics production runs calculated for whole protein.

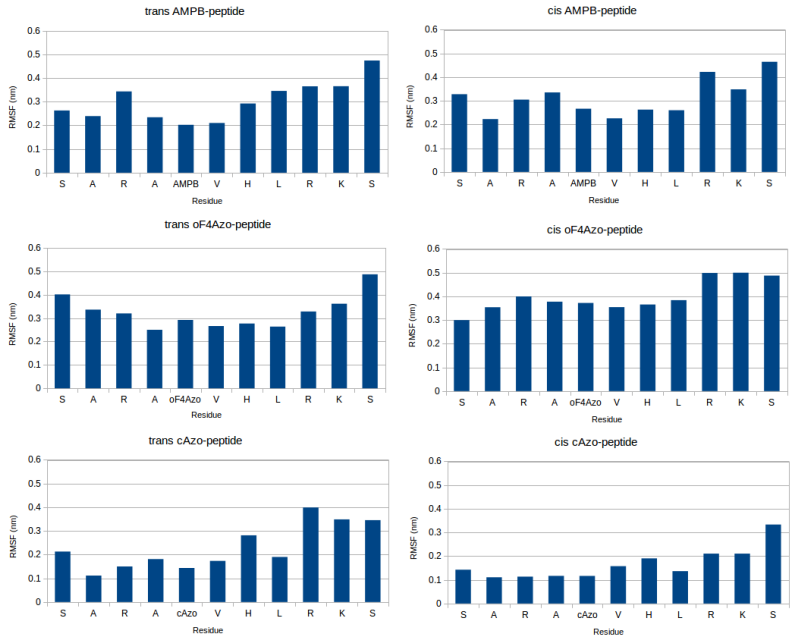

Figure S31. Fluctuations of residues from peptidomimetics expressed as root mean square fluctuations (RMSF) during 20 ns of molecular dynamics simulations.

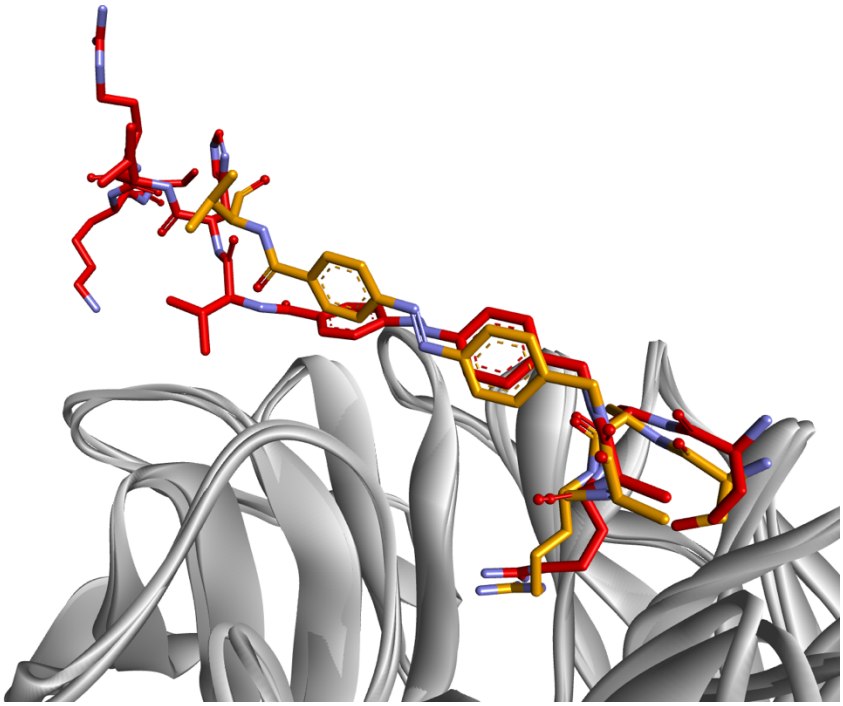

Figure S32. Comparison between binding modes of *trans* **AMPB-peptide** (**3**) predicted in MD simulation (red) and the described in the crystal structure PDB code: 5M23 (orange).

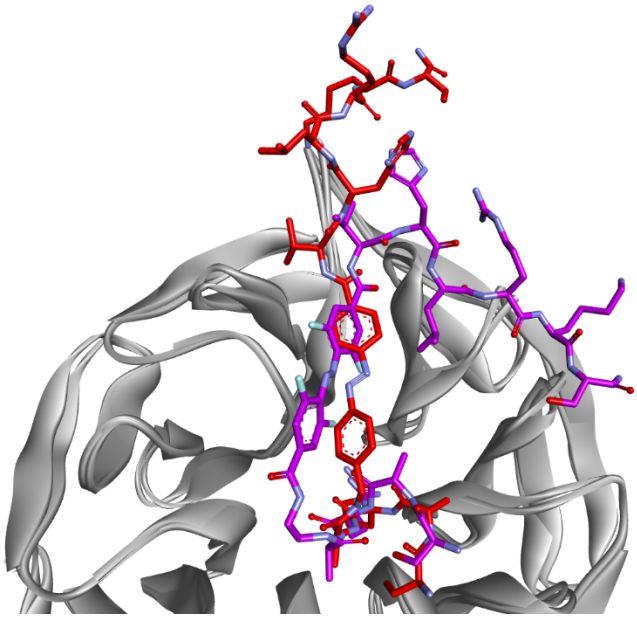

Figure S33. Comparison between binding modes predicted in MD simulations for *trans* **AMPB-peptide** (**3**) (red) and for *trans* **oF_4Azo-peptide** (**5**) (dark purple).

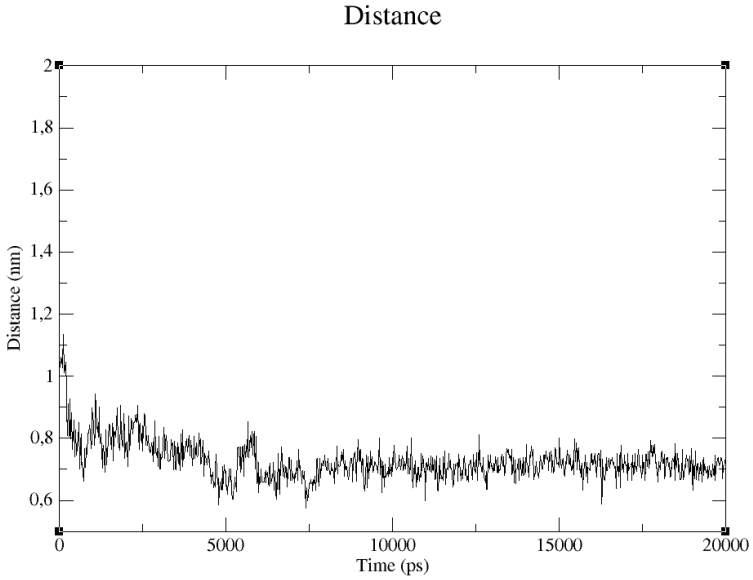

Figure S34. Measured distances between leucine of *trans* **oF_4Azo-peptide** (**5**) (-VHLRKS sequence of peptides) and tetra-*ortho*-fluoroazobenzene during 20 ns of simulation. Stabilization of intramolecular interaction was achieved after 7 ns.

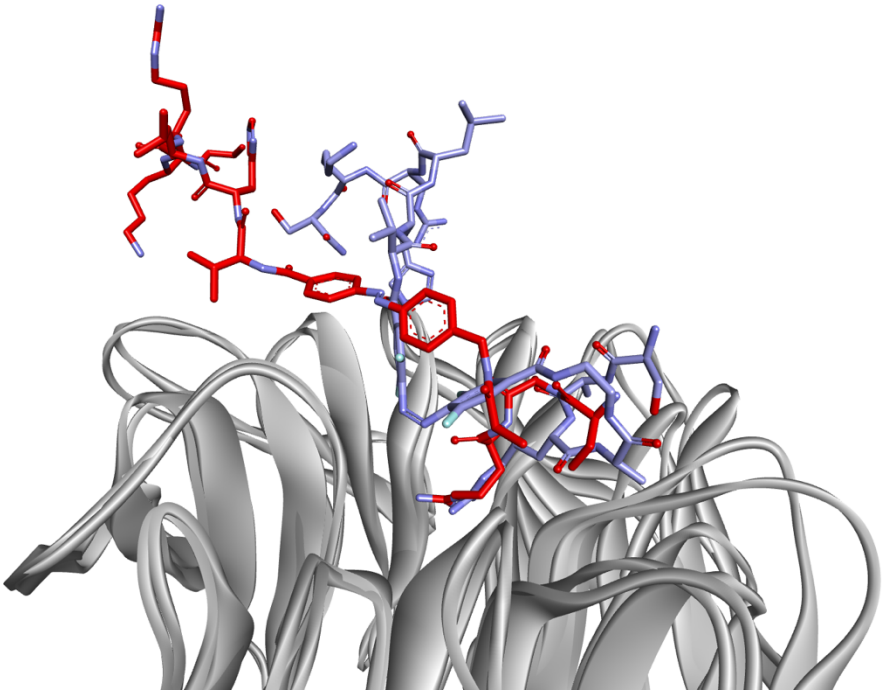

Figure S35. Comparison between binding modes predicted in MD simulations for *trans* **AMPB-peptide** (**3**) (red) and for *cis* **oF4Azo-peptide** (**5**) (light purple).

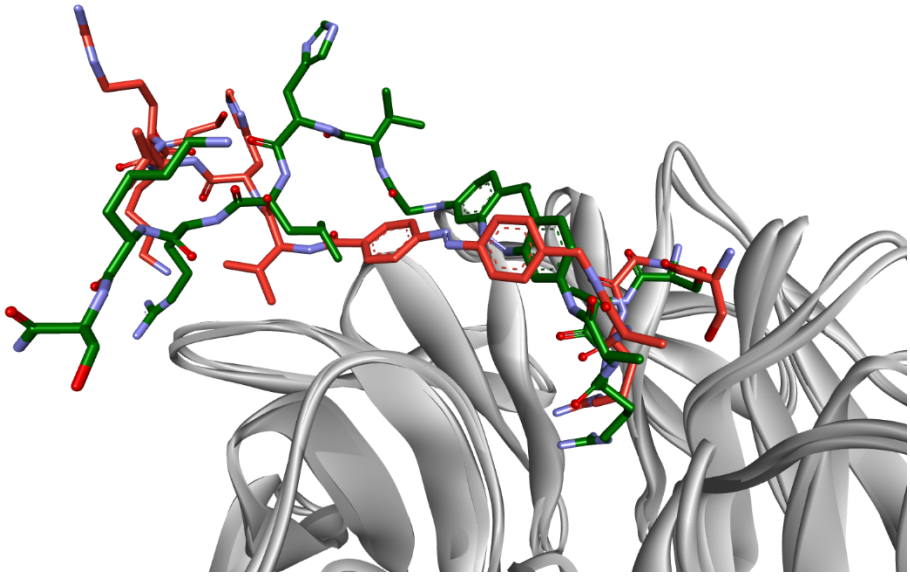

Figure S36. Comparison between binding modes predicted in MD simulations for *trans* **AMPB-peptide** (**3**) (red) and for *trans* **cAzo-peptide** (**4**) (dark green).

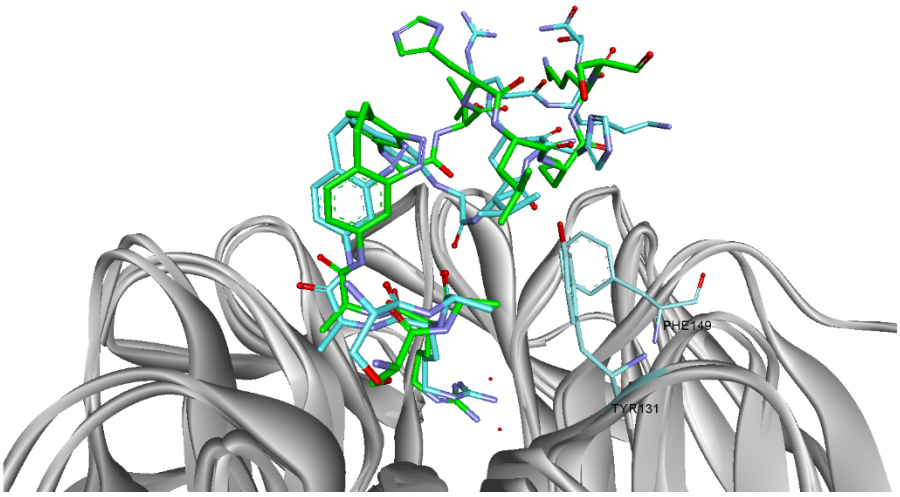

Figure S37. Comparison between binding modes of *cis* **cAzo-peptide (4)** computationally predicted (turquoise) and the described in the crystal structure PDB code: 6IAM (green).

Table S3. Average and standard deviation for RMSD values through 20 ns of MD runs.

ID	Average	Standard Deviation
trans **AMPB-peptide** (**3**)	0.080306	0.017255
cis **AMPB-peptide** (**3**)	0.213613	0.034478
trans **oF4Azo-peptide** (**5**)	0.214039	0.04802
cis **oF4Azo-peptide** (**5**)	0.224058	0.033466
trans **cAzo-peptide** (**4**)	0.221753	0.033309
cis **cAzo-peptide (4)**	0.243952	0.086662

Table S4. Surface area of protein-peptidomimetics binding surface calculated by Volaera.[17]

ID	Binding surface area (Å^2)
trans **AMPB-peptide** (**3**)	2153.999
cis **AMPB-peptide** (**3**)	1643.134
trans **oF$_4$Azo-peptide** (**5**)	1617.568
cis **oF$_4$Azo-peptide** (**5**)	1533.619
trans **cAzo-peptide** (**4**)	1827.268
cis **cAzo-peptide** (**4**)	1287.747

References

[1] C. Knie, M. Utecht, F. Zhao, H. Kulla, S. Kovalenko, A. M. Brouwer, P. Saalfrank, S. Hecht, D. Bléger, *Chem. - A Eur. J.* **2014**, *20*, 16492–16501.

[2] R. Sjöback, J. Nygren, M. Kubista, *Spectrochim. Acta Part A Mol. Biomol. Spectrosc.* **1995**, *51*, L7–L21.

[3] L. Albert, J. Xu, R. Wan, V. Srinivasan, Y. Dou, O. Vázquez, *Chem. Sci.* **2017**, *8*, 4612–4618.

[4] Z. Nikolovska-Coleska, R. Wang, X. Fang, H. Pan, Y. Tomita, P. Li, P. P. Roller, K. Krajewski, N. G. Saito, J. a. Stuckey, et al., *Anal. Biochem.* **2004**, *332*, 261–273.

[5] H. Sell, C. Näther, R. Herges, *Beilstein J. Org. Chem.* **2013**, *9*, 1–7.

[6] D. Bleger, J. Schwarz, A. M. Brouwer, S. Hecht, *J. Am. Chem. Soc.* **2012**, *134*, 20597–20600.

[7] D. Bléger, S. Hecht, *Angew. Chemie - Int. Ed.* **2015**, *54*, 11338–11349.

[8] D. Chouikhi, M. Ciobanu, C. Zambaldo, V. Duplan, S. Barluenga, N. Winssinger, *Chem. - A Eur. J.* **2012**, *18*, 12698–12704.

[9] W. J. Fang, T. Yakovleva, J. V. Aldrich, *Biopolymers* **2011**, *96*, 715–722.

[10] W. S. Hancock, J. E. Battersby, *Anal. Biochem.* **1976**, *71*, 260–264.

[11] R. S. Molday, S. W. Englander, R. G. Kallen, *Biochemistry* **1972**, *11*, 150.

[12] Y. Bai, J. S. Milne, L. Mayne, S. W. Englander, *Proteins* **1993**, *86*, 75–86.

[13] Y. Zhang, Y. Paterson, H. Roder, *Protein Sci.* **1995**, *9*, 804–814.

[14] N. Hayashi, H. Kuyama, C. Nakajima, K. Kawahara, M. Miyagi, O. Nishimura, H. Matsuo, T. Nakazawa, **2014**, Biochemistry, *53*, 1818–1826

[15] M. Kielmas, J. Adamczyk, *Anal. Bioanal. Chem.* **2014**, *406*, 8013–8020.

[16] A. C. Wallace, R. A. Laskowski, J. M. Thornton, *Protein Eng.* **1995**, *8*, 127–134.

[17] J. V. Ribeiro, J. A. C. Tamames, N. M. F. S. A. Cerqueira, P. A. Fernandes, M. J. Ramos, *Chem. Biol. Drug Des.* **2013**, *82*, 743–755.